SRI International

(2)

Final Report • February, 1993

KINETICS AND ENERGY TRANSFER IN NONEQUILIBRIUM FLUID FLOWS

David R. Crosley
Molecular Physics Laboratory

SRI Project 1262
Contract No. DAAL03-90-K-0001

MP 93-004

Prepared for:

U.S. Army Research Office
P.O. Box 12211
Research Triangle Park, NC 27709-2211

Attn: Patsy Ashe

• (415) 326-6200 • FAX (415) 326-5512 • Telex 334486

REPORT DOCUMENTATION PAGE

Form Approved OMB No. 0704-0188

1. AGENCY USE ONLY *(Leave blank)*	2. REPORT DATE	3. REPORT TYPE AND DATES COVERED
	February 3, 1993	Final 17 Jun 90 - 16 Sep 92

4. TITLE AND SUBTITLE
Kinetics and Energy Transfer in Nonequilibrium Fluid Flows

5. FUNDING NUMBERS
DAAL03-90-K-0001

6. AUTHOR(S)
David R. Crosley

7. PERFORMING ORGANIZATION NAME(S) AND ADDRESS(ES)
SRI International
Molecular Physics Laboratory
333 Ravenswood Avenue
Menlo Park, California 94025

8. PERFORMING ORGANIZATION REPORT NUMBER

9. SPONSORING/MONITORING AGENCY NAME(S) AND ADDRESS(ES)
U.S. Army Research Office
P.O. Box 12211
Research Triangle Park, NC 27709-2211

10. SPONSORING/MONITORING AGENCY REPORT NUMBER
ARO 27864.3-CG-SDI

11. SUPPLEMENTARY NOTES
The view, opinions and/or findings contained in this report are those of the author(s) and should not be construed as an official Department of the Army position, policy, or decision, unless so designated by other documentation.

12a. DISTRIBUTION/AVAILABILITY STATEMENT
Approved for public release, distribution unlimited.

12b. DISTRIBUTION CODE

13. ABSTRACT *(Maximum 200 words)*

Chemical kinetics and energy transfer have been investigated for nonequilibrium fluid flow. The particular process of interest is ultraviolet emission from the $A^2\Sigma^+$ excited electronic state of NO, which is generated under nonequilibrium conditions in the bow shock waves of ascending missiles at 50 to 100 km altitude. A literature survey of the pertinent rate constants and mechanism for use in computer models of the process has been undertaken. Emission from NO has been studied in shock tubes, using shock heated air and other gas mixtures. Collisional quenching of the $A^2\Sigma^+$ state is the reverse of heavy particle excitation of the emission. Its temperature dependence has been studied in a heated cell and a shock tube. An attempt was made to determine the final vibrational state distribution in the ground electronic state, concluding that the NO is transferred into high vibrational levels.

14. SUBJECT TERMS			15. NUMBER OF PAGES 16
			16. PRICE CODE
17. SECURITY CLASSIFICATION OF REPORT UNCLASSIFIED	18. SECURITY CLASSIFICATION OF THIS PAGE UNCLASSIFIED	19. SECURITY CLASSIFICATION OF ABSTRACT UNCLASSIFIED	20. LIMITATION OF ABSTRACT UL

CONTENTS

ABSTRACT

Chemical kinetics and energy transfer have been investigated for nonequilibrium fluid flow. The particular process of interest is ultraviolet emission from the $A^2\Sigma^+$ excited electronic state of NO, which is generated under nonequilibrium conditions in the bow shock waves of ascending missiles at 50 to 100 km altitude. A literature survey of the pertinent rate constants and mechanism for use in computer models of the process has been undertaken. Emission from NO has been studied in shock tubes, using shock heated air and other gas mixtures. Collisional quenching of the $A^2\Sigma^+$ state is the reverse of heavy particle excitation of the emission. Its temperature dependence has been studied in a heated cell and a shock tube. An attempt was made to determine the final vibrational state distribution in the ground electronic state, concluding that the NO is transferred into high vibrational levels.

INTRODUCTION

Nonequilibrium Effects in Fluid Flow

Under conditions of high velocity and low pressure, the time scale for energy transfer and chemical rate processes in gases can become comparable to flow times. Finite kinetic rate processes lead to nonequilibrium excited state (vibrational and electronic state) population distributions as well as nonequilibrium chemical compositions, and these nonequilibrium chemical kinetics effects can play a significant role in determining the characteristics of fluid flow. Not only are such phenomena of considerable fundamental interest in chemical physics, but they also can govern the behavior of real systems to such an extent that it is very important to have a working knowledge of their effects.

The effects of nonequilibrium flow on radiative and convective heat transfer rates in spacecraft reentry have been well known (although not well understood) for a long time. Such effects also influence the pressure distributions around flight vehicles and thus alter their aerodynamic stability characteristics. This lesser known effect caused an unexpected variation in the reentry flight properties of the space shuttle.[1] Nonequilibrium chemical kinetics effects are extremely important in the current Project Pathfinder program (aero-assisted orbital transfer using aerodynamic braking, and manned Mars mission studies) and the National Aerospace Plane program. In the latter program, nonequilibrium chemistry is important not only in the external flowfield but in the hydrogen/air combustion chemistry of the scramjet propulsion system as well.

Nonequilibrium energy transfer and finite chemical reaction rates are important in understanding the details of most combustion processes, including propellant performance for guns and rockets. External flowfield issues will be important in setting altitude and performance limits for the SDI's kinetic kill vehicles and for future tactical hypersonic projectiles and missiles. Historically, nonequilibrium chemical effects have played a major role in the radiative properties of rocket plumes, including both base heating of the rocket itself and the observability of the plume in the infrared and ultraviolet spectral regions. Finally, nonequilibrium chemical kinetics govern the ultraviolet radiative emission in shock-heated air and thus the observability of bow-shock radiation from rockets and missiles. The last topic has been the specific focus of our current program.

The recognition of these effects is not new; it was driven initially by the nuclear weapons program and later by the strategic missile and space programs of the late 1950s and 1960s. Much of our knowledge to date rests on shock tube observations made during that latter period; much excellent work was done, but the effort did not persist long enough, nor were the diagnostic tools good enough to resolve many issues. Thus, the questions have been handled problematically, usually by a phenomenological description covering some given range of conditions of translational temperature and pressure. It is unclear how to extrapolate such treatments to describe other situations of interest, particularly those not amenable to laboratory investigation. Recent technological advances, however, have made possible fresh attacks on the problem of nonequilibrium effects in fluid flow. The first is the use of highly sophisticated optical techniques, often involving lasers and new detectors, to study directly molecules in nonequilibrium distributions. The second is the use of advanced computational methods to obtain realistic theoretical predictions of nonequilibrium behavior at the molecular level and to model complex reacting systems involving nonequilibrium effects and detailed fluid mechanics.

Ultraviolet Radiation in Boost Phase and Reentry

Our program has concentrated on understanding nonequilibrium effects on the ultraviolet emission observed in both boost phase and reentry of missiles. Two flights have been made to observe and test our understanding of the mechanism forming this radiation.[2] Bow Shock 1, flown in April 1990, concentrated largely on the NO γ band system emitted during ascent, while the rocket climbed from 40 to 80 km altitude at a speed of 3.5 km/s. Bow Shock 2, undertaken in February 1991, had two objectives. One was the observation of the NO radiation at the higher speeds achievable during reentry, extending it to 5 km/s at an altitude at the upper end of the range of Bow Shock 1. The second goal was the observation of the rocket plume region, i.e., viewing backwards along the rocket. In addition to blackbody and AlCl molecular plume emission during firing, CO Cameron bands were observed during a time period following burnout.[3,4]

The NO γ band radiation is emitted by the $A^2\Sigma^+$ state, formed in the bow shock with the rarefied atmosphere at these altitudes. The CO Cameron bands, emitted by the metastable $a^3\Pi$ state, occur either directly from the rocket plume or in the plume-atmosphere interaction. In either case, kinetics and thermodynamic nonequilibrium effects dominate the flowfields in which the excited states are formed. Although translational and rotational equilibrium is likely obtained on a local scale, vibrational states do not have time to equilibrate and the electronically excited states are probably formed through very quantum-state-specific energy transfer or chemical reaction steps.

Attempts have been made to model the γ band formation by using a flowfield code[5] incorporating the NEQAIR mechanism for excited NO formation.[6] This latter code was assembled primarily to understand reentry of space vehicles at much higher speeds than encountered here, and thus it emphasizes electron excitation mechanisms. Heavy particle excitation is treated approximately, and choices had to be made for parametrizing the chemical effects of nonequilibrium vibrational distributions. A sensible choice is the use of two temperatures to reflect this nonequilibrium.[7] However, this approach leads to an underprediction of the altitude dependence of the radiance by several orders of magnitude.[5] The use of a single temperature throughout is inappropriate on physical grounds but nonetheless produces predictions in much better agreement with experiment. Thus, our phenomenological model for the conditions of the tests is missing some information on basic nonequilibrium kinetics involved in NO(A) formation and such information is still necessary for reliable extrapolation and use of modeling results.

OBJECTIVES AND APPROACH

Our effort in this project began with a comprehensive literature search and critical review of rate constants, together with computer modeling of reaction kinetics, vibrational relaxation, electronic state excitation, and energy transfer processes to evaluate formation, excitation, and removal processes for these species.[8] The best recommendations for reliable rate constants were made, and crucial gaps in our understanding were identified. From the model, the most likely processes populating the emitting states were selected. Plans for the future research include updating this work to evaluate likely mechanisms in the high altitude, higher speed reentry flight planned for the near future and considering the effects of CO_2 and H_2O as track species in the vehicle environment.

The experimental thrusts have been of three types. The first, a direct examination of NO γ band emission in air heated in a laboratory shock tube, led to conclusions similar to those obtained in experiments at Calspan.[9] The second was an investigation of the quenching of the $A^2\Sigma^+$ state of NO, in an attempt to understand quantitatively the removal and reverse collisional excitation mechanism under shock-heated conditions. The temperature dependence of quenching was investigated in a heated cell[10] and in a shock tube.[11] The vibrational state distribution of ground state NO following the quenching process was investigated, and we began a quantitative study of the radiative properties and rates of the $B^2\Pi$ state of NO, which emits the β band system also observed in the same wavelength region.

RESEARCH PERFORMED

Critical Review and Modeling of Mechanisms and Kinetics

The first part of our study was a survey of the current kinetics treatments of radiating, shock-heated air, together with a critical review of reaction and energy transfer rates for high temperature air. The conditions considered were those appropriate to the bow-shock radiation problem: 3-4 km/s velocity and 30-70 km altitude. The assumptions made were reviewed, and the best available energy transfer and reaction rate constants recommended (with comments regarding uncertainties in those values). A simplified computer model of the appropriate physical and chemical processes involved was assembled to help identify the main mechanistic routes as well as the sensitive parameters. (The modeling of nonequilibrium vibrational relaxation was not treated in this survey.) We briefly summarize the conclusions below.

Recommended rate constants, in three-parameter form, for the relevant reactions of N_2, O_2, N, O, and NO were presented.[8] These should be reliable up to temperatures of 4000 K and good to within perhaps a factor of two to 6000 K. The situation is poorer for NO decomposition, for which case the rate constants have factor-of-two uncertainties to 4000 K. Several processes were considered for the formation of electronically excited NO in the highly energetic mixture of N_2, O_2, N, O, and NO. Formation of the emitting A-state from ion-electron recombination can clearly be ruled out. Electron impact excitation is probably a minor process under the conditions considered, although it plays a much larger role at higher temperatures where there are more electrons. N + O atomic recombination probably contributes, but the most likely excitation processes are energy transfer from metastable N_2 $A^3\Sigma_u^+$ molecules and direct collisional excitation by collisions of ground-state NO with atoms and molecules. The importance of this last process, the reverse of electronic quenching, is highly uncertain owing to lack of knowledge of the vibrational and electronic state branching distribution in the quenching process.

The heavy-particle collisional excitation process would normally be thought of and calculated as the equilibrium reverse of the known quenching rate. However, this approach does not generally apply under the nonequilibrium conditions of shock-heated gases; it would apply only if the products of quenching for both gases are in partial equilibrium with the entire ensemble of each molecule. It thus becomes crucial to determine the final state products of the quenching event in order to evaluate the significance of the collisional excitation mechanism. This need motivate one of our proposed experiments described below.

The most widely used code for calculating the radiative part of the kinetics of shock-heated air is the NEQAIR code of Park.[6] Since this code was designed for the temperatures found in reentry problems, which are higher than those of interest here, electron impact excitation of radiating states was emphasized. In accordance with our recommendations, an improved version of the excitation mechanism was inserted into the code used for emission predictions,[5] and it was found that heavy-particle collisional excitation was a potentially important radiative excitation mechanism at lower temperatures. As we have just pointed out, there is considerable uncertainty in the rates assumed for that process because of the lack of information on the final products of quenching.

This portion of the project was concluded with the publication of a report[8] detailing our recommendations and conclusions and distributed to the community involved in the questions of radiating, shock-heated air and related issues of nonequilibrium effects in fluid flow.

Shock Tube Experiments

Preliminary shock tube experiments were performed, partially in preparation for more sophisticated laser-based diagnostic measurements and partially to directly investigate the spectral and temporal evolution of NO radiative emission at high temperature and low pressure. The stainless steel shock tube has a 5-cm ID and is 4.6 m long with a 1.3-m driver section; it was operated with cold helium or hydrogen driver gas to produce shock velocities up to ~5 km/s at p_1 = 0.5 torr (corresponding to 50 km altitude). Since we had not operated at such conditions before, this effort was aimed partly at establishing just what shock speeds could be achieved. Establishing the duration of test time behind the shock wave is also of concern when operating at low test pressures and high velocities. By measuring the 308-nm emission from OH generated when the H_2 driver gas reacts with O_2 from the test gas at the contact interface, we were able to determine that, at the conditions cited above, the test duration is approximately 20 μs. Unfortunately, this test duration does not allow full relaxation of the ultraviolet emission to its equilibrium level, although we can still study the nonequilibrium region with its critical kinetic processes.

Our primary diagnostic tool to date has been time-resolved detection of emission bands following the arrival of the incident shock wave at the observation windows. The test station has four ports in a cruciform arrangement. Two ports are fitted with uv windows, 1-mm wide slits separated by 10 or 30 mm to provide good spatial resolution, and photomultiplier tubes with selected bandpass filters. A third port, also fitted with a uv window, provides line-of-sight access to a spectrometer/optical multichannel analyzer (OMA) detection system. The fourth port has a piezoelectric pressure transducer (PCB Model 112A21), which has a 5.5-mm diameter and less

than 2-μs rise time and thus serves to determine the shock arrival time at the slit positions with less than 1 μs uncertainty. This accuracy was confirmed by using a HeNe laser with a 2-mm-diameter beam in conjunction with a position-sensitive detector to measure the shock arrival at the same location by the laser schlieren technique. The laser schlieren signal showed that the initial rise of the pressure transducer signal corresponded to the shock arrival at the observation point.

We have thus far concentrated on monitoring emissions at 225 ± 11.5 nm and 311 ± 6 nm. The former wavelength coincides with the NO(A,v = 0 → X,v = 0) band, while the latter coincides with both the NO(B,v=0→X,v=7) band and the OH(A,v = 0 → X,v = 0) band. At p_1 = 0.5 torr and U_S = 4.6 km/s, the signals for both wavelengths rise to a peak in less than 2 μs and then decrease on a time scale on the order of 20 μs. We attribute these signals to NO γ- and β-band emissions. The 310-nm signal then increases to a much higher maximum that we attribute to OH emission produced by combustion of the hydrogen driver in the air; this late increase signals the end of the usable test time. The shapes of these intensity histories are in agreement with the recent results of Wurster et al.[9] However, because we have a shock detector situated exactly at the observation station, it is perhaps easier for us to correlate the intensity profiles more precisely with the shock location.

The spectrally resolved shock tube experiments emphasized the spectral and temporal evolution of NO radiation emission at high temperature and low pressure.[11] In this case, the shock tube was operated with cold He or H_2 driver gas to produce shock velocities up to 5 km/s and a pressure corresponding to 50 km altitude. The spectral distributions and the time shapes of the intensity histories at 255 and 311 nm are in agreement with the similar shock tube measurements of Wurster et al., [9] but we were unable to observe significant emission localized in the nonequilbrium portion of the shock. By using mixtures of different gases, such as NO seeded into pure N_2, O_2, or N_2O, we were able to observe that collisional effects on the excited state played a significant role in determining the amount of γ band emission.

Temperature Dependence of NO Quenching

A quantitative understanding of the emission of electronically excited NO requires knowledge of collisional rates for both excitation and deexcitation (quenching) processes. A nearly universal assumption about such rates is that the cross sections for quenching are independent of temperature. Recent experiments, however, have shown that quenching cross sections of diatomic hydrides are controlled by attractive forces and show a significant decrease with increasing temperature.[12] Quenching cross sections for NO $A^2\Sigma^+$ at room temperature are large (10-100 $Å^2$ for gases of atmospheric interest), suggesting the influence of attractive forces

here also. However, no quenching cross sections for NO at elevated temperatures were previously available, and so we have performed such measurements.

Quenching cross sections were measured by monitoring the temporal evolution of laser-induced fluorescence from excited NO. The excited state decays faster as the pressure of added collider is increased. Both the $A^2\Sigma^+$ and $B^2\Pi$ states were studied, using both a filtered photomultiplier and monochromator to spectrally disperse the fluorescence. The A-state was pumped via two-photon absorption near 453 nm, and the B-state by one-photon transitions near 220 nm. The measurements were made in a slowly flowing cell that could be externally heated to 750 K; temperatures were measured *in situ* using LIF excitation scans of rotational level populations.

Cross sections were determined for the colliders NO, O_2, N_2, and H_2O. The room temperature results for $A^2\Sigma^+$ were in excellent agreement with previous determinations. N_2 shows very small quenching, but the cross sections for the other three gases are large. Quenching by H_2O exhibits a decrease with increasing temperature, dropping from 105 $Å^2$ to 37 $Å^2$ between 300 and 750 K. Cross sections for NO and O_2 were constant at 37 and 21 $Å^2$, respectively. In the $B^2\Pi$ state, quenching by both NO and H_2O decreases with increasing temperature over this same range.

Our general experience with the temperature dependence of quenching for other molecules indicates that quenching cross sections tend to level off above ~800 K. Thus, the present measurements cover the most important temperature range, and we can assume that the current measured cross section values for NO at 750 K form the best recommended estimate for use in shock-heated air radiation calculations. This assumption is corroborated for water by the flame measurements of Cattolica et al., at 1100 K.[13]

When the B-state was pumped, emission from the A-state was also seen. The yield of $A \rightarrow X$ emission relative to $B \rightarrow X$ was pressure-dependent, which indicates a collisional mechanism for $B \rightarrow A$ transfer occurring to some extent (~5%) for every collider studied. When the A state γ-band emission is time-resolved, it can be fit to the sum of two exponentials, one corresponding to the decay of the B-state that fills A and the other representing the decay of A. However, the pressure-dependence of the time constants for those exponentials is incompatible with direct transfer and suggests an intermediate state. In this same energy region lies the metastable $a^4\Pi$ state, which could serve as such a reservoir.

These results have important implications for the question of radiative emission from NO in shock-heated air. A significant drop in quenching cross section with increasing temperature, as seen here, could greatly alter the predicted relative importance of the heavy-particle collisional

mechanism assumed in the NEQAIR code[6] as the excitation pathway. It would also change somewhat the predicted removal rate and thus the steady-state concentration of NO($A^2\Sigma^+$). If NO(A) is formed by transfer from N_2 $A^3\Sigma_u^+$, the $B^2\Pi$ and metastable $a^4\Pi$ states are likely involved, and collisional energy transfer among these three states will be important in determining the yield of emission in a given spectral interval.

More generally, the variation in the temperature dependence of quenching among different colliders cannot be explained by a simple, uniform picture of the collision dynamics. Although attractive force interactions are clearly implied by the large size of the cross sections, the mechanisms are more complex and need separate examination for each collider. This problem has clear ramifications regarding the many simplifying assumptions that must be used in parametric, phenomenological treatments of energy transfer in nonequilibrium flows.

The heated cell experiments also showed that the self-quenching of NO was independent of temperature. We investigated this quenching process at the much higher temperature attainable in a shock tube.[11] The nature of the shock tube experiment permitted us to fire the laser only once during the shock event, so each datum was recorded using excitation from a single laser pulse, which led to relatively large error bars. Measurements were made at one temperature (3500 K) and two pressures each of NO and the background gas N_2. The results indicated a cross section larger than that obtained at room temperature, but the overlap is within the 30% 2-σ error bars in the shock tube experiment.

Perhaps the most surprising result of these first high temperature shock tube quenching experiments was the finding that at high temperature the N_2 molecule quenched the $A^2\Sigma^+$ of NO with a relatively large cross section of 2 $Å^2$. This cross section is two to three orders of magnitude larger than that found at room temperature, where quenching by N_2 is negligible. It has important implications for collisional effects not only in the bow-shock experiments but also in laser-induced fluorescence flame diagnostics[14] for NO.

Before these experiments, the quenching of NO had never been investigated above room temperature, despite its considerable importance. Following these pioneering heated cell and shock tube approaches to quenching, two subsequent experiments elsewhere have made a comprehensive study of NO quenching at many temperatures for a large variety of colliders (predominantly those important in hydrocarbon flames). A heated cell study[15] went up to 1700 K, while the shock tube investigation[16] approached the range of our shock tube measurements. Agreement was found in all cases. The high temperature dependence of quenching of $A^2\Sigma^+$ NO is now well established for many colliders.

Final State Of Quenching Of NO

Although cross sections for collisional quenching of electronically excited states have been measured for many colliders, very little is known about the disposition of the large amount of electronic energy lost during the process. Most likely, markedly nonthermal distributions are produced among electronic, vibrational, and rotational degrees of freedom. Under such nonequilibrium conditions, one cannot use the principle of microscopic reversibility to calculate the important upward electronic excitation rates from the readily measured excited state loss rates, because detailed balancing, with its use of a temperature, implicitly assumes a single thermal distribution over all degrees of freedom. When a nonequilibrium distribution holds, the calculation of upward rates must include both the state-by-state nonequilibrium population distribution, and each state specific rate constant for the downward process. This experiment was undertaken to provide the information needed to deal with the nonequilibrium situation.

In a cell at room temperature, the $A^2\Sigma^+$ state of NO was prepared using excitation from a tuned, pulsed laser. Enough NO was added that about half the excited state population radiated and the other half was quenched by collisions with the NO itself. After a time delay of about 1 μs, long enough to ensure that quenching had occurred but too short for significant vibrational relaxation, a second laser was fired. Tuned to transitions of either the A-X or the B-X electronic systems, this second laser was used to probe the final state distribution following the quenching event.

In the first series of experiments, copious signal levels were seen, exhibiting a large range of vibrational levels and individual rotational and spin-orbit levels within each. (The time scales and pressures were such that the rotational levels are expected to be at thermal equilibrium, in agreement with experiment.) Only a semiquantitative measure of relative vibrational levels could be obtained. However, a large range of approximately equally populated vibrational levels was found, from $v = 6$ to $v = 24$, the limits of the search.

These results had a significant implication for the bow-shock mechanism, assuming that the quenching colliders in the bow-shock environment (N_2, O_2, and atoms) produce a final state distribution like the NO measured here. If each vibrational level is equally populated in the quenching process, only about 3% of the quenched molecules are found in any one vibrational level of the X state. Thus, if a large fraction of the NO molecules formed in the bow shock are in, say, $v = 0$ to 2 (i.e., vibrationally cold), the upward transfer cross section is only about 10% of that calculated using detailed balance and the measured downward quenching rate. This cross section is similar to that estimated in the code used to calculate the bow-shock radiation.

Subsequent experiments at higher sensitivity have now shown that these first results are in error. For equivalent conditions, the signal levels were found to be a factor of 100 smaller than found in the first set of experiments, for vibrational levels in the range v = 14 to 25. After considerable effort, we have concluded that the previous experiments were contaminated by the presence of NO_2 in the gas cell. The NO_2 may have been present in the original gas cylinder, or it may have formed photolytically in the slowly flowing mixture. Previous work at SRI[17] showed that photolysis of NO_2 at wavelengths similar to that of the pump laser produces vibrationally excited NO product. Although we cannot prove conclusively that this occurred in the original experiments, it is the only realistic explanation for the observation of highly vibrationally excited NO in that work.

We then turned to a renewed investigation of the NO(X) levels populated following NO(A) excitation and collision with NO. We could conveniently observe populations in the levels between v = 3 and 10. The measured distribution is very similar to the A-X, v' = 0 Franck Condon pattern, indicating that all or most of the levels are populated by radiation and not directly from quenching.

O_2 was then added as a quencher and NO(X) levels were observed as a function of collider pressure. The distribution observed in this case was slightly different although restricted to the lower levels and thus still due in large part to population resulting from radiation.

We conclude that the majority of the quenched NO is transferred to very high-lying vibrational levels, above those observable with the available laser wavelengths, and that a negligible amount is directly transferred to the lowest levels. However, this new result now indicates that the heavy particle excitation mechanism (determined for NO on NO) is much slower than that assumed in the code for N_2-NO collisions and probably does not contribute to the formation of emitting NO $A^2\Sigma^+$ molecules in the bow shocks.

Radiative Properties of the NO $B^2\Pi$ State

The primary component of emission from NO in the bow-shock experiments is that in the γ bands, but spectral fits indicate radiation from high temperature air in laboratory experiments includes the β, δ, and ε bands as well.[18] We have thus begun an investigation of the radiative properties of the $B^2\Pi$ state, which radiates the β bands.

The experiment is straightforward, although it must be carried out carefully to produce high quality data. A laser is used to excite the B state, and the resulting β band emission is detected with a spectrometer. Scanning the spectrometer furnishes intensities of each vibrational band. These are then compared with Franck-Condon factors computed with an RKR program to

obtain empirical values of the electronic transition moment. This method furnishes an excellent test of that moment, which can in turn be used to calculate the intensities of many vibrational bands over any wavelength range or temperature of interest.

Thus far, experiments have been performed on the v' = 7 level, excited by an ArF excimer laser at 193 nm. The excited level partially overlaps the v'= 0 level of the $C^2\Sigma^+$ state, which must be separated in the fluorescence. Because of the much shorter lifetime of the C state, the separation can be performed using detection electronic gating delayed about 100 ns after the laser pulse. Furthermore, the pressure must be kept very low to avoid energy transfer that populates other vibrational levels of B, or levels of the A state, which radiate in the ultraviolet region.

Results have been obtained showing fluorescence out to v = 26 of the ground electronic state, following excitation of v' = 7 of B. (These bands and analysis were also used in the probe step study of final states of quenching discussed above). The results agree with the general form of the electronic transition moment deduced from emission of a distribution of B state vibrational levels in a microwave discharge.[19] These were compared with *ab initio* calculations made at NASA Ames.[20,21]

PUBLICATIONS AND PRESENTATIONS

The following publications have resulted from work done on this project:

1. G. P. Smith, D. R. Crosley, and D. J. Eckstrom, "Mechanism and Rate Constants for the Chemistry of Radiating, Shock-Heated Air," SRI International Report MP 89-037, (February 1989). (Appendix A)

2. G. A. Raiche and D. R. Crosley, "Temperature Dependent Quenching of the $A^2\Sigma^+$ and $B^2\Pi$ States of NO," J. Chem. Phys. **92**, 5211 (1990). (Appendix B)

3. U. E. Meier, G. A. Raiche, D. R. Crosley, G. P. Smith, and D. J. Eckstrom, "Laser-Induced Fluorescence Decay Lifetimes of NO $A^2\Sigma^+$ in a Shock Tube," Appl. Phys. B **53**, 138 (1991). (Appendix C)

4. D. R. Crosley, "Laser Measurement of Reactive Intermediates in Combustion.," in *Turbulence and Molecular Processes in Combustion,* T. Takeno, Ed. (Elsevier, Amsterdam, 1992), in press. (Appendix D)

The following conference presentations (with published abstracts) have been made:

1. G. A. Raiche, G. P. Smith, and D. R. Crosley, "Temperature Dependent Energy Transfer in NO ($A^2\Sigma^+$, $B^2\Pi$): 300-750K," Fifth Interdisciplinary Laser Science Conference, Stanford, California, August 1989 [Bull. Am. Phys. Soc. **34**, 1682 (1989)].

2. G. A. Raiche, G. P. Smith, and D. R. Crosley, "Temperature Dependent Quenching of NO $A^2\Sigma^+$ and $B^2\Pi$ by H_2O," 42nd Annual Gaseous Electronics Conference, Palo Alto, California, October 1989.

3. G. A. Raiche, G. P. Smith, and D. R. Crosley, "Temperature Dependence of Energy Transfer in NO $A^2\Sigma^+$ and $B^2\Pi$," Western States Meeting of the Combustion Institute, Livermore, California, October 1989.

4. D. R. Crosley, "Collisional Quenching and Relaxation in Laser Detection of Atmospheric Radicals," American Chemical Society Meeting, Washington, DC, August 1990 [invited].

5. U. E. Meier, G. A. Raiche, D. R. Crosley, G. P. Smith, and D. J. Eckstrom, "Emission Spectra and LIF Decay Lifetimes of NO in Shock Tubes," Western States Meeting of the Combustion Institute, La Jolla, California, October 1990.

6. U. E. Meier, L. E. Jusinski, and D. R. Crosley, "Ground State Vibrational Distribution Following Collisional Quenching of NO ($A^2\Sigma^+$, v'=0)," Twelfth International Conference on Molecular Energy Transfer, Nijmegen, The Netherlands, July 1991.

7. G. A. Raiche, U. E. Meier, D. R. Crosley, G. P. Smith, and D. J. Eckstrom, "Laser Induced Fluorescence Decay Lifetimes of Shock-Heated NO $A^2\Sigma^+$," Seventh Interdisciplinary Laser Science Conference, Monterey, California, September 1991 [Bull. Am. Phys. Soc. **36**, 1951 (1991)].

8. D. R. Crosley, "Laser Measurement of Chemically Reactive Intermediates in Combustion," Sixth Toyota Conference, Mikkabi, Japan, October 1992 [invited].

9. D. R. Crosley, "Chemistry and Energy Transfer in Flames and Shocks," Second International Symposium on High Temperature and Combustion Chemistry, Tokyo, Japan, October 1992 [invited].

In addition, the project supported contributed presentations at the Gordon Conference on Molecular Energy Transfer at Wolfeboro, New Hampshire, in July 1989 and the Gordon Conference on Laser Diagnostics in Combustion at Plymouth, New Hampshire in July 1989. It also supported both invited and contributed presentations at the Gordon Conference on Laser Diagnostics in Combustion at Plymouth, New Hampshire, in July 1991.

REFERENCES

1. C. S. Park, NASA Ames Research Center, private communication.

2. D. A. Levin, L. H. Caveny, D. M. Mann, R. J. Collins, C. Howlett, P. Espy, P. Erdman, and E. Zipf, 19th JANNAF Exhaust Plume Technology Conference, May 1991.

3. G. Candler, D. Levin, J. Brandenburg, R. Collins, P. Erdman, E. Zipf, and C. Howlett, AIAA Paper 92-0125, Aerospace Sciences Meeting, January 1992.

4. P. Erdman, University of Pittsburgh, private communication.

5. D. A. Levin, G. V. Candler, R. J. Collins, R. W. Erdman, E. Zipf, P. Espy, and C. Howlett, AIAA Paper 91-1411, Thermophysics Conference, June 1991.

6. C. Park, Prog. Astro. Aero. **96**, 395 (1985).

7. C. Park, Prog. Astro. Aero. **96**, 511 (1985).

8. G. P. Smith, D. R. Crosley, and D. J. Eckstrom, SRI International Report MP89-037, SRI International, Menlo Park, California (February 1989).

9. W. H. Wurster, C. E. Treanor, and M. J. Williams, AIAA Paper 89-1918, Fluid Dynamics, Plasma Dynamics, and Lasers Conference, June 1989.

10. G. A. Raiche and D. R. Crosley, J. Chem. Phys. **92**, 5211 (1990).

11. U. E. Meier, G. A. Raiche, D. R. Crosley, G. P. Smith, and D. J. Eckstrom, Appl. Phys. B **53**, 138 (1991).

12. D. R. Crosley, J. Phys. Chem. **93**, 6273 (1989).

13. R. J. Cattolica, T. G. Mataga, and J. A. Cavalowsky, J. Quant. Spectr. Rad. Trans. **42**, 499 (1989).

14. D. E. Heard, J. B. Jeffries, G. P. Smith, and D. R. Crosley, Comb. Flame **88**, 137 (1992).

15. M. C. Drake and J. W. Ratcliffe, General Motors Research Laboratory Report GMR-7426 (July 1991).

16. J. A. Gray, P. H. Paul, and J. L. Durant, Chem. Phys. Lett. **190**, 266 (1992).

17. T. G. Slanger, W. K. Bischel, and M. J. Dyer, J. Chem. Phys. **79**, 2231 (1983).

18. C. O. Laux, S. Moreau, and C. H. Kruger, AIAA Paper 92-2969 (1992).

19. L. G. Piper, T. R. Tucker, and W. P. Cummings, J. Chem. Phys. **94**, 7667 (1991).

20. D. M. Loope, J. Quant Spect Rad Trans. **27**, 459 (1982).

21. S. R. Langhoff, H. Partridge, L. W. Bauschlicher, and A. Komornicki, J. Chem. Phys. **94**, 6638 (1991).

Appendix A

MECHANISM AND RATE CONSTANTS FOR THE CHEMISTRY OF RADIATING, SHOCK-HEATED AIR

February 8, 1989

Interim Assessment

MECHANISM AND RATE CONSTANTS FOR THE CHEMISTRY OF RADIATING, SHOCK-HEATED AIR

By: Gregory P. Smith, David R. Crosley,
and Donald J. Eckstrom

Prepared for:

ARMY RESEARCH OFFICE
Research Triangle Park, NC 27709-2211
Attn: Dr. David M. Mann

SRI Project No. 6277
Contract No. F33615-87-C-2763
Report MP 89-037

I. INTRODUCTION

This report briefly summarizes the processes relevant to the formation of emitting, electronically excited NO in shock heated air, and recommends rate constants for use in modeling these processes. It is the result of a search and evaluation of the literature in the field, undertaken as Phase I of an SRI International contract with the Army Research Office, as part of SDIO's Bowshock Radiation Program. The major goal of this effort was the identification of important and uncertain areas of the chemistry controlling ultraviolet NO emissions, in order to design appropriate shock tube experiments to help resolve such questions. Thus some of the values will be improved later, and hence these recommendations therefore should not be considered the final word. Nevertheless, they should be considered by modelers as checks of potentially serious deficiencies in their rate constants or mechanisms. In turn, modeled experiments may indicate problems with some of the recommended values.

The following discussion is divided into three parts: air chemistry rate constants, basic rate constants relevant to the problem of vibrational disequilibrium, and processes for the production of excited A-state NO. The discussion will be brief and non-comprehensive, and will focus on what we have identified as the most important processes. In particular, modeling alternatives for treating the case of vibrational disequilibrium will not be treated here and are left to other references. There are large uncertainties in the rate constants associated with most of the final category, which describes the radiation-producing chemistry. (see Park) [Pa85] Finally, these recommendations only apply to the range of conditions relevant to the bow shock radiation problem, 3-4 km/s velocity and 30-70 km altitude. Some rate constants may require re-examination for other areas of hypersonic air chemistry and radiation, such as the aerospace plane and re-entry phenomena.

II. RATE CONSTANTS FOR HIGH TEMPERATURE AIR CHEMISTRY

Reactions and recommended three parameter rate constant expressions for high temperature air chemistry are given in Table 1. Reverse rate constants should be automatically included via the equilibrium constant (recall the equilibrium constant is the ratio of forward and reverse rate constants, available from JANAF). We do not consider the problem of differing translational and vibrational temperatures. Units are $cm^3/mole/s$ ($cm^6/mole^2/s$ for termolecular reactions), with T in kelvins and the activation energy in calories. Sources refer to the reference list. Rate constants for collisionally activated processes such as dissociation reactions, those involving "M" in Table 1, include enhanced collision efficiencies on the following line for those species with substantially faster rate constants than the standard N_2. The majority of the neutral reaction rate constants are taken from the review and evaluation of Baulch and colleagues.[BDH72]

Rate constants for the ionic processes are adopted from the DNA Handbook.[BB72] These ionic reactions are generally fast, and serve to scramble charge rapidly. The predictions of models will thus be relatively insensitive to the rates, although the set must be included above ~6000K, where NO^+ is no longer necessarily the dominant equilibrium ion.

There are, from examination of model calculations and sensitivity analysis for the appropriate conditions, five main reactions responsible for most of the chemistry:

$$O_2 + M \rightarrow O + O + M \quad (1)$$

$$O + N_2 \rightarrow NO + N \quad (2)$$

$$N + O_2 \rightarrow NO + O \quad (3)$$

$$NO + M \rightarrow N + O + M \quad (4)$$

$$N + O \rightarrow NO^+ + e^- \quad (5)$$

These are oxygen decomposition, followed by the Zeldovich chain chemistry to create NO, NO decomposition, and associative ionization. Nitrogen decomposition is relatively

unimportant in our time and temperature range. The reverse reactions are also implicitly included via the equilibrium constants.

Rate constants for the first three reactions can be considered fairly accurately known, since there are reliable rate constant measurements at least up to 4000K in either the forward or reverse direction. We adopt Baulch's value[BDH72] for argon as the collider, M, for nitrogen also since its behavior is similar in other cases. We also use his recommendations for oxygen atoms and molecules as collider gas, M. The O_2 value is probably appropriate for NO as well. The value for electrons as collider M is estimated by scaling the collision rate by a reduced mass factor, but that reaction is not important here. Estimated accuracy for reaction (1) is within a factor of two up to 8000K. The Zeldovich rate constants, reactions (2) and (3), are taken from a more recent review by Hanson [HS84] incorporating his own modern shock tube measurements, and are also accurate to within a factor of two for temperatures below 6000K.

The situation is poorer for NO decomposition. Three sets of data in the 4000-7000K range disagree by consecutive factors of four or more.[HS84] Recent measurements at lower temperatures by Thielen and Roth[TR84] support older values of Wray and Teare[WT62] that fall in the middle range of the conflicting data. We reject the lowest values (see Hanson for a discussion) and recommend an average between Wray and Koshi's more recent measurement.[KBS79] This should be viewed with greater uncertainty, since high temperature NO decomposition is plagued by secondary reactions and non-equilibrium effects which must be deconvoluted from the measurements. For collider efficiencies we use the measured argon value for the diatomic molecules, and by analogy to the oxygen decomposition results triple this for O and N atomic colliders. Finally, reported decomposition efficiencies for NO collider are 20 times the argon number,[KBS79,WT62] a value totally at variance with normal kinetics experience. We have compromised here to a factor of 10 enhancement, but we estimate very large error bars as a result.

In addition, a second NO assisted decomposition reaction is included in the table. This is an abstraction reaction forming N_2O and O.[BDH72] Since N_2O decomposes rapidly,[BDH72] we choose to write the products as $N_2 + O + O$ to avoid adding another species, and the reaction is written to be irreversible ($\rightarrow$ instead of = in Table 1). This is a minor channel.

Lastly, the associative ionization reaction that produces the electrons is written from the opposite direction. The DNA discussion[BB72] and recommendation is adopted. This

extends the measured lower temperature data by using the theoretical calculation of Bardsley.[Ba62] This is in accord with satellite data[Zi88], but does exceed some shock tube results at higher temperatures. Planned measurements may improve this situation.

Given the factor of two or more uncertainty in these rate constants, and the desired level of predictive accuracy, the use of rate constants in existing codes within 50% of those recommended here can probably be considered adequate. The values in Candler' s code for reactions 1-5 fall within these limits, while the parameters of Park[Pa87] for decomposition reactions 1 and 4 appear faster than the recommendations, and tnat for the ionization reaction (-5) is slower. Since some of the reactions are entered in the reverse direction, care should also be taken to insure that the equilibrium constant expressions are consistent with the JANAF table values. Modelers are encouraged to recheck input data in this connection.

Some rate constants are also given in Table 2 for those atmospheric reactions responsible for producing CN and OH, since prominent ultraviolet emissions have also been observed from these species. These rates are less certain, and will not be discussed further at this time.

III. THERMAL DISEQUILIBRIUM AND VIBRATIONAL ENERGY TRANSFER

In the previous section, we discussed the thermodynamic nonequilibrium caused by the slow evolution of the kinetics. A second type of nonequilibrium also exists, under which the system cannot be characterized by a single temperature - a situation we will distinguish by the term thermal disequilibrium for clarity. Under many conditions, the time required to transfer energy from initially excited translation (T) and rotation (R) into vibration (V) is comparable to the kinetics. The simplest treatment, recommended for its relative ease of adoption, is to use two temperatures, translational-rotational and vibrational-electronic. Even this is approximate, since the electronic/electron temperature may lag the vibrational temperature, and in many cases the actual vibrational distribution cannot be characterized as Boltzmann.

The first question concerns which temperature to use for the rate constants of Table 1, mainly the key reactions 1-5. Current practice generally uses the translational temperature for the Zeldovich reactions 2 and 3 [Pa87,Pa88] pending further theoretical information [Ja86]. Reaction 5 will only depend on translational energy. Dissociation reactions 1 and 4 clearly depend on climbing the vibrational ladder, although translational energy plays a role in the final dissociative step, and Jaffe[Ja86] has shown that rotational energy can suppress the barrier for dissociation. Current practice [Pa88] is to use the geometric mean of the two temperatures for the dissociation reactions. The reverse recombination reactions can only depend on the translational temperature, however.

The current hybrid temperature approach for the time being is probably a fair approximation for this case where thermal disequilibrium is severe only at early times. As has been pointed out, [Pa88] care must be exercised in both energy transfer and dissociation to conserve energy. At no time, according to the second law of thermodynamics, should values of the vibrational temperature exceed the translational temperature, although both may exceed the final equilibrium temperature before the kinetics are complete.

The second main question is how fast energy is transferred from translation to vibration, since this affects the dissociation process. Models to describe this situation will not be discussed, other than to note that one of the newer, advanced, yet computationally

tractable efforts is that of Park.[Pa87,Pa88] This two temperature treatment is recommended at this time. The kinetics input to such models is some basic V-T rate constant, typically the relaxation rate constant for v=1. In addition, V-V rates between diatomics are needed.

Lewis and Treanor[LT74] have compiled the pre-1974 data, and little additional high temperature work has appeared since. We have evaluated these results and produce a list of recommended Arrhenius parameters in Table 3, valid over a temperature range of 2000-8000 K. (The use of an Arrhenius form is for convenience. The more exact treatment of vibrational energy transfer rate constants uses the form $\log(k)=A+BT^{-1/3}$.) Species labeled by (1) are the v=1 levels. Reverse V-V rate constants were determined by adding the vibrational energy difference to the activation energy. The rate constant for NO relaxation by oxygen atoms comes from a more recent measurement by Glanzer and Troe.[GT75] Note the lack of most V-T rates between non-identical diatomics; this is due to the dominance of V-V processes in most experiments of this type. There are some upper limits available, although they are not listed in Table 3.

IV. RADIATION KINETICS - MECHANISM OF NO(A) FORMATION

The most important deficiencies and uncertainties are in knowledge of the kinetics that control the NO radiation itself. A variety of mechanisms for NO excitation and de-excitation must be considered. The most frequently used steady-state treatment[Pa85] considers electron impact excitation as the primary process, and in addition appears to predict too small a value for the experimentally observed emissions. We will deal with some less severe conditions under which this process will be relatively unimportant, and for which the current code has not been validated. The excitation processes are electron impact excitation, atomic association, ion-electron recombination, heavy particle excitation, and energy transfer from metastable nitrogen:

$$NO + e^- \rightarrow NO(A) + e^- \quad (6)$$

$$N + O\,(+M) \rightarrow NO(A)\,(+M) \quad (7)$$

$$NO^+ + e^-\,(+M) \rightarrow NO(A) + e^-\,(+M) \quad (8)$$

$$NO + M \rightarrow NO(A) + M \quad (9)$$

$$NO + N_2(A) \rightarrow NO(A) + N_2 \quad (10)$$

In order to evaluate the role of (10), we also must consider the production and loss mechanisms for the excited metastable triplet nitrogen A-state. The major loss processes for NO(A) will be radiative emission and collisional quenching, which includes collisional dissociation. Finally, since the NO beta bands are also seen in emission, B-state excitation must also be considered.

A. ELECTRON IMPACT, ATOMIC ASSOCIATION, AND RADIATIVE RECOMBINATION

Electron impact excitation cross sections for the NO gamma bands have been measured[IB75] from v"=0 to the first three vibrational levels of the A-state as a function of electron energy. Using the Franck-Condon principle (normally applied to photon excitation) and appropriate threshold energy shifts, excitation rate constants from higher

vibrational levels of the ground state can be calculated at high temperatures. This is done in Park's code.[Pa85] A rate constant calculated this way for 5000K is given in Table 4. It is difficult to estimate the error in this value, because it is very sensitive to behavior in the threshold region, and we have simply chosen a linear extrapolation from the first measured point (6eV) back to the thermodynamic threshold (5.5eV). Unfortunately, no similar cross sections exist for the B state, and current practice[Pa85] has been the use of the same values for the A state as a generic approximation. The current recommended procedure appears adequate.

The atomic association rate constants(7) for NO excited state production have been measured for both A and B states by Gross and Cohen[GC68] up to 1500K. The mechanisms involve both collisional and collision-free paths, and are quite complex. We adopt their temperature dependent expressions (for nitrogen as collider) for use at much higher temperatures. Given this complexity, the amount of extrapolation, and the difficulty of the experiments, the possibility of considerable error must be entertained. This uncertainty includes possible enhanced rates for non-nitrogen third body colliders.

Electron-ion radiative recombination(8) was examined, both without and with third body collisional stabilization. The rate constants are estimates given in the DNA handbook,[BB72] based solely on limited data involving atoms. Here it has been necessary to assume a branching ratio into the A-state, and we have chosen the reasonable value of 10%. This mechanism will turn out to be insignificant under typical conditions for bow shock heated air.

B. COLLISIONAL EXCITATION BY ATOMS AND MOLECULES

Collisional excitation, process (9), is the reverse of A-state quenching to the ground state and is related to it by equilibrium. This rate constant (9) can be calculated using the equilibrium constant and the quenching rate constant if we know the fraction of the quenching that produces both NO and the quencher molecule or atom in their ground states. To the extent that quenching produces other final states that are not in equilibrium with the ground state, the above argument does not hold. This treatment automatically includes near-resonant vibrational-to-electronic transfer from highly excited vibrational levels. An examination of the quenching rate constants for NO(A) determined by Ravishankara[GR87] together with the appropriate equilibrium constants predicts large rates for collisional excitation, if the above condition of ground state products is met even 5% of the time.

Thus an informed judgment must be formulated for NO(A) formation by this mechanism. There are quartet states of NO nearby energetically to the A-state, and they are known to be collisionally connected.[GC68] Also, NO(A) is near the dissociation limit to atoms and does predissociate from higher vibrational levels. This suggests that very little, if any, ground state NO product will result from A-state quenching at high temperatures. Thus our current, provisional recommendation includes no collisional excitation of this nature. However, given the large amounts of ground state NO formed chemically, the presence of even a modest fraction of the partial equilibrium amount of NO(A) formed by this mechanism (that is, a modest fraction of quenching to the ground states) would be significant.

Specific comments can be made for some of the quencher molecules, as potential collisional activators. N_2 has a low quenching rate constant, and thus the reverse process of producing NO(A) is clearly insignificant for any conditions. Both NO and O_2 as quenchers have other electronic states possible as products of quenching (including dissociation to atoms). If those quenching channels dominate, then the equilibrium reverse treatment for collisional activation does not apply and (9) is not significant.

A measurement of these final state distributions in NO(A) quenching by NO and O_2 colliders is needed to assess qualitatively the amount of heavy particle direct excitation. Although it appears that this is not a major route, it would be significant if even a modest return to the lowest levels is found experimentally.

It is also possible for the quartet states to serve as a "dark" reservoir for gamma band emission. However, rapid subsequent collisional dissociation from these quartets is more likely. A-state production through the quartets as intermediates is already implicitly treated in the complex kinetics of the measured atom association rate constant. (The reverse of (7), quenching to form N + O atoms, i.e., collisional dissociation from NO(A), is also treated therein.) It is clear, both from the Gross and Cohen paper and references there-in, as well as from this brief description, that NO excited state collision kinetics are very complex, and this precludes a precise state-by-state treatment at this time.

C. ENERGY TRANSFER FROM $N_2(A)$

The final NO excitation mechanism to be considered involves energy transfer from the metastable triplet A-state of N_2. The full treatment of this mechanism requires excitation rates for $N_2(A)$, $N_2(A)$ loss rates by collisional quenching, and an energy transfer rate constant to form NO(A). We consider the latter two related points first. We

have adopted the quenching rate constants given by Golde[Go88] in his review, noting that N_2 itself is an ineffective quencher. No temperature dependence is used, in line with our general experience for quenching rate constants and the temperature independence found by Slanger[SWB73] for rapid quenchers of $N_2(A)$. However, there is some data for N atoms at very high temperature which suggest this particular rate may be 50% lower at high temperature than the 300 K value listed in Table 4.[FA72] The second question is the fraction of the total quenching rate for $N_2(A)$ by NO which produces NO(A) as the product. Piper[PCR86] has made measurements at 300K. These values suggest that 90% or more of the collisions lead to production of NO(A) in v=0, with very little production in higher vibrational levels or in the B state of NO. Large rates also exist for higher vibrational levels of $N_2(A)$, suggesting little temperature dependence.[PCR86] Thus we will adopt a branching fraction of 100% into NO(A), and no production of NO(B), following energy transfer from $N_2(A)$. This affords a strong mechanism for NO(A) production. We also include the reverse reaction.

In actuality, the nascent vibrational distribution produced in the NO A-state in the shock heated air itself may provide clues to the origin of the excitation. For example, the possibility that the Franck-Condon principle governs the direct collisional excitation by heavy particles can be studied experimentally. Electron impact excitation appears to be described by Franck-Condon factors, and from cold NO would produce ratios of 1:1.7:2.5 in v=0, 1, and 2 respectively. Production from $N_2(A)$ would produce predominantly v=0 in NO(A). If the production is by inverse predissociation (atomic association, $N + O \rightarrow$ NO(A)), we should also find NO produced primarily in the B state v=0 and 3, and the C state v=0, through pathways involving the a and b quartet states. Although determining such vibrational distributions through dispersed, vibrationally resolved emission measurements is not easy due to band overlap, this could be a key to sorting out the important excitation mechanisms under different conditions.

Next, the $N_2(A)$ production mechanisms must be treated in a manner analogous to reactions (6)-(9) for NO above. Electron impact cross sections are available from the data of Cartwright.[CTC77] In this case, the effect of populating higher nitrogen ground state vibrational levels at high temperatures results in a large increase in A-state excitation due to more favorable Franck-Condon overlaps at lower electron excitation energies. For the atomic association process, $N + N \rightarrow N_2(A)$, both direct and third-body processes are incorporated. The direct rate constant uses the measurement of Young and Black,[YB66] with the same temperature dependence which Gross and Cohen measured for N + O. The three-body expression for A-state production is Appleton's theoretical value at high

temperatures.[SAK70] This has been partially verified by matching experiments at lower temperatures where ground state nitrogen production was measured. In the same way we ruled out ion-electron recombination (8) for the NO case, we dismiss this mechanism as a significant A-state nitrogen source for our conditions. Finally, we consider collisional activation. Molecular nitrogen itself is too slow to be significant (see the discussion of $N_2(A)$ quenching by N_2 above).[GR87] Since quenching by oxygen atoms produces $O(^1S)$ at 4 eV, and molecular oxygen is dissociated in the quenching, [Go88] the reverse equilibrium processes involving ground state oxygen collisional excitation do not apply (see the NO(A) discussion). NO most surely should behave similarly to O_2 as a quencher. Ground state N atoms however have been shown to be efficient $N_2(A)$ quenchers at high temperatures,[FA72] and thus the reverse collisional activation step for N alone must be included. (Note that Setser[MSS70] contends that a significant fraction of the product of this quenching is $N(^2P)$, rather than the ground state. To the extent that $N(^2P)$ is the product, and the extent that $N(^2P)$ is not in equilibrium with the ground state, collisional activation will be lessened.)

The foregoing discussion suggests that a comprehensive, accurate treatment of collisional activation and quenching mechanisms requires a large manifold of excited state populations, especially for metastables such as NO quartets, $O(^1S)$, $O(^1D)$, $N(^2D)$, etc. Consideration of such a full mechanism is beyond the scope of current evaluation and knowledge.

D. NO(A) LOSS MECHANISMS

The radiative lifetime and quenching rates for NO(A) will then combine to give the NO gamma band fluorescence quantum yields. Molecular rate constants for NO(A) quenching are from Ravishankara's data at 300K,[GR87] with the same assumed lack of a temperature dependence. The atom values are estimated. The important quenchers are O_2, O, and NO. The question of NO(A) (and $N_2(A)$) removal at high temperatures requires closer examination. We assume that the efficient thermal quenching mechanisms represented by our chosen rate constants continue to dominate at higher collision energies; however, even a change or addition of a new mechanism for the quenching is incapable of increasing already large rate constants very much. The situation may be different for molecular nitrogen, a poor 300K quencher. Park's NEQAIR code[Pa85] considers NO(A) removal by collisional dissociation to N + O, with an activation energy equal to the 1 eV endothermicity. At 5000K, this gives total quenching rates larger than the conventional approach here. This 1 eV barrier is most likely too low, because NO(A) does not directly

correlate to the ground state atoms, and must therefore take an indirect route to dissociation. One possible route through a curve crossing involving the quartet state potentials raises this activation energy to 2.5 eV.

The kinetics relevant to NO(A) production and loss are summarized in Table 4. The table lists reactions, sources for the rate constants, the rate constant at 5000K (in cm^3/mole/sec), the reaction rate for excited state production or loss under typical conditions (in molecules/cm^3/sec), and the coefficients for the rate constant expression (in the same form as in Table 1).

E. SUMMARY

Table 4 provides some perspective on the relative importance of these processes under a typical condition of temperature, pressure, and composition found in shock heated air. We use this to suggest what should be included, and to see what processes deserve further scrutiny, not to predict actual results. The production and loss rates are also shown in Table 4 at 0.5 atmospheres (the pressure after shock compression), 5000K temperature, and a composition (mole fractions) of 0.155 O_2, 0.764 N_2, 0.035 NO, 0.048 O, 0.0005 N, and 1.2×10^{-6} ionization. (These concentrations are taken from a computer model of the kinetics, with values at 10 microseconds after the shock. A positive rate indicates production of the excited state shown on the right hand side of the reaction, while a negative rate indicates destruction of the excited state shown on the left hand side.) Electron impact, which plays the dominant role at higher temperatures, is less important an NO(A) source than the association. Ion-electron recombination is safely neglected. Energy transfer from metastable nitrogen appears to play a major role, even if the production mechanism for $N_2(A)$ is restricted to only electron impact and not atomic collisional activation. Thus energy transfer and atomic association appear to dominate the NO(A) excitation mechanisms at these conditions. Unfortunately, the rate constants governing those processes are the least well known.

V. COMPARISONS AND CONCLUSIONS

The widely used current code for calculating the radiation part of the kinetics is the NEQAIR code of Park.[Pa85] It was designed to describe re-entry conditions, with higher temperatures and velocities than important here. Thus electron impact excitation was emphasized. In order to extend its applicability to the shock heated air problems of present interest, modifications and additions need to be made. The NEQAIR code uses a quasi-steady state approach, but currently does not accommodate all of the kinetics suggested above. As listed in the most recent version, electron impact excitation, de-excitation, and dissociation; heavy collider induced dissociation, excitation, and quenching; and radiative decay are included. The heavy collider rates, however, are only approximated by uniform 1 A^2 cross-sections. Thus quenching and atomic recombination to excited states with the Gross and Cohen rate constants are not being treated correctly. The potentially important $N_2(A)$ mechanism is not included and will be more difficult to incorporate. Changes addressing these omissions must be made in order to extend the applicability of this code to conditions of lower temperature and ionization. In addition, recent measurements at SRI[GS89] indicate the NO(B) radiative lifetime is a factor of two shorter than previous values. This will increase the predicted beta band emission by a factor of two.

Conditions under which the well-treated electron impact excitation mechanism no longer dominates will be encountered in the bow shock problem. Therefore, it is important to incorporate these mechanisms and the best available rate constants into the radiation calculation. Use of the correct chemical rate constants and thermodynamics should be verified. The rate constants of Gross and Cohen(GC) for $N + O \rightarrow NO(A)$, which includes both collision free and collisionally stabilized components, should be explicitly included. The $N_2(A)$ energy transfer mechanism needs to be added. Experimentally determined quenching rate constants should be used, although the correct treatment of the reverse process of collisional excitation remains unclear at this time. Finally, it is important to ensure that the collision induced dissociation rate constants currently used for NO(A) do not exceed the equilibrium reverse of the pressure dependent portion of the Gross and Cohen rate constant, nor should they dominate the NO(A) quenching. Despite the remaining uncertainties, such changes in current codes based on fundamental

measurements are needed if the predictive capabilities of these codes are to be extended to the lower temperatures prevalent in the bow shock environment.

Table 1. Recommended Rate Constants

$k=AT^n\exp(-E/kT)$

Reaction	Source	A(cm^3/mole)	n	E(cal)	
$O_2 + M = O + O + M$	[BDH72]	1.800E+18	-1.0	118760.	(1)
e= 160.x (enhanced collision efficiencies)					
$O_2 + O_2 = O_2 + O + O$	[BDH72]	9.800E+24	-2.5	118760.	(1)
$O_2 + O = O + O + O$	[BDH72]	3.500E+25	-2.5	118760.	(1)
$N_2 + M = N + N + M$	[BDH72]	3.700E+21	-1.6	226400.	
N= 4.x O= 4.x e= 160.x					
$NO + M = N + O + M$	[WT62]	2.300E+17	-0.5	148000.	(4)
NO= 10.x O= 3.x N= 3.x e= 160.x					
$NO + NO - N_2 + O + O$	[BDH72]	1.300E+12	0.0	64200.	
$O + N_2 = NO + N$	[HS84]	1.800E+14	0.0	76740.	(2)
$O + NO = N + O_2$	[HS84]	3.810E+09	1.0	41640.	(-3)
$NO^+ + e = N + O$	[BB72]	2.300E+18	-.40	0.0	(-5)
$O_2^+ + e = O + O$	[BB72]	1.670E+20	-.63	0.0	
$N_2^+ + e = N + N$	[BB72]	1.500E+18	-.39	0.0	
$O^+ + e + M = O + M$	[BB72]	1.120E+27	-2.5	0.0	
N_2= 3.x O_2= 3.x NO= 3.x e= 2.x					
$N^+ + e + M = N + M$	[BB72]	1.120E+27	-2.5	0.0	
N_2= 3.x O_2= 3.x NO= 3.x e= 2.x					
$NO^+ + e + M = NO + M$	[BB72]	3.370E+27	-2.5	0.0	
$O_2^+ + e + M = O_2 + M$	[BB72]	3.370E+27	-2.5	0.0	
$N_2^+ + e + M = N_2 + M$	[BB72]	3.370E+27	-2.5	0.0	
$N_2^+ + NO = NO^+ + N_2$	[BB72]	2.000E+14	0.0	0.0	
$N_2^+ + O_2 = O_2^+ + N_2$	[BB72]	5.100E+07	1.4	0.0	
$N_2^+ + O = O^+ + N_2$	[BB72]	2.100E+11	.41	0.0	
$N_2^+ + N = N^+ + N_2$	[EST]	6.000E+11	0.0	0.0	
$N^+ + NO = NO^+ + N$	[BB72]	5.000E+14	0.0	0.0	
$N^+ + O_2 = O_2^+ + N$	[BB72]	1.400E+12	.57	0.0	
$N^+ + O = O^+ + N$	[BB72]	6.000E+11	0.0	0.0	
$O^+ + NO = NO^+ + O$	[BB72]	3.250E+06	1.66	0.0	
$O^+ + O_2 = O_2^+ + O$	[BB72]	8.300E+08	1.2	0.0	
$O_2^+ + NO = NO^+ + O_2$	[BB72]	2.700E+14	0.0	0.0	
$O^+ + N_2 = NO^+ + N$	[BB72]	5.330E+05	2.0	0.0	
$N^+ + O_2 = NO^+ + O$	[BB72]	1.400E+12	.57	0.0	
$O_2^+ + N = NO^+ + O$	[BB72]	7.200E+13	0.0	0.0	
$N_2^+ + O = NO^+ + N$	[BB72]	1.000E+13	.18	0.0	

Table 2. Rate Constants Involving CN and OH

$O + CO_2 = CO + O_2$	[BDH75]	1.700E+13	0.0	53000.
$CO + M = C + O + M$	[BDH75]	8.800E+29	-3.52	257400.
$CN + M = C + N + M$	[BDH75]	2.000E+14	0.0	150000.
$4+ CN = N + CO$	[LH84]	2.000E+13	0.0	420.
$C + NO = CN + O$	[BGL75]	6.300E+11	0.5	0.0
$C + N_2 = CN + N$	[BGL75]	1.300E+12	0.5	45500.
$H_2O + M = OH + H + M$	[BDH72]	3.500E+15	0.0	105800.
$O + H + M = OH + M$	(EST)	5.000E+14	0.0	0.0
$O + H_2O = OH + OH$	[BDH72]	6.800E+13	0.0	18480.
$H + O_2 = OH + O$	[BDH72]	2.200E+14	0.0	16900.

Table 3. Simple T-V, V-V Treatment

(one way reactions, equilibrium not implicitly used)

		A	E
$NO(1) + N_2 \rightarrow N_2(1) + NO$	(EQ)	3.240E+13	17100.
$N_2(1) + NO \rightarrow NO(1) + N_2$	(LT74)	3.240E+13	15800.
$NO(1) + O_2 \rightarrow O_2(1) + NO$	(EST)	3.240E+13	15800.
$O_2(1) + NO \rightarrow NO(1) + O_2$	(EQ)	3.240E+13	16715.
$O_2(1) + N_2 \rightarrow N_2(1) + O_2$	(EQ)	1.000E+12	18015.
$N_2(1) + O_2 \rightarrow O_2(1) + N_2$	(LT74)	1.000E+12	15800.
$N_2(1) + N_2 \rightarrow N_2 + N_2$	(LT74)	1.800E+13	43200.
$N_2(1) + O \rightarrow N_2 + O$	(LT74)	3.000E+11	6800.
$N_2(1) + N \rightarrow N_2 + N$	(EST)	3.000E+11	6800.
$O_2(1) + O_2 \rightarrow O_2 + O_2$	(LT74)	5.400E+12	21000.
$O_2(1) + O \rightarrow O_2 + O$	(LT74)	6.000E+12	6800.
$NO(1) + NO \rightarrow NO + NO$	(LT74)	3.800E+12	10520.
$NO(1) + O \rightarrow NO + O$	(GT)	1.500E+12	0.0

Table 4. NO(A) Excitation

Reaction	Source	coefficients	k(5000)	rate
$e + NO \rightarrow NO(A) + e$	IB75	-------	2.20E+08	7.5E+12
$N + O \rightarrow NO(A)$	GC68	5.2E7,-.35,0.	2.65E+06	5.2E+13
$N + O + M \rightarrow NO(A) + M$	GC68	9.0E16,-1.24,0.	2.33E+12	5.3E+13
$NO^+ + e \rightarrow NO(A)$	EST	1.3E13,-.7,0.	3.35E+10	4.0E+10
$NO^+ + e + M \rightarrow NO(A) + M$	EST	5.6E26,-2.5,0.	3.24E+17	4.4E+11
$N_2 + e \rightarrow N_2(A) + e$	CTC77	-------	7.20E+08	5.4E+14
$N + N \rightarrow N_2(A)$	YB66	4.9E7,-.35,0.	2.60E+06	5.3E+11
$N + N + M \rightarrow N_2(A) + M$	SAK70	4.6E20,-1.6,0.	5.50E+14	1.3E+14
$N + N_2 \rightarrow N_2(A) + N$	SAK70	9.2E21,-2.23,145000.	2.60E+07	8.1E+15
$N_2(A) + NO \rightarrow NO(A) + N_2$	PCR86	4.0E13,0.,0 -1.6E+6	4.00E+13	4.8E+17
$NO(A) + N_2 \rightarrow N_2(A) + NO$	EQ	2.4E14,0.,18000.	4.00E+13	-3.5E+7
$N_2(A) + M \rightarrow N_2 + M$	Go88	1.4E12,0.,0.	1.44E+12	-1.3E+6
N_2=0. O_2=1.x O=12.5x N=21.x e=250.x				
$NO(A) + M \rightarrow NO + M$	GR87	8.4E13,0.,0.	8.40E+13	-3.2E+7
N_2=0.0 O_2=1.x O=2.x NO=2.3x e=1.6x				
$NO(A) \rightarrow NO + h\nu$	ZHW76	4.7E7,0.,0.	4.65E+07	-4.7E+7

Note:
Rate constant coefficients A,n,E in the form $k=AT^n\exp(-E/RT)$.
Rate constant units $cm^3/mole/s$ or $cm^6/mole^2/s$.
Rates give are for production of the excited state species on the right side of the reaction, under the conditions given in the text, in units of $molecules/cm^3/s$.
Negative rates refer to loss of the excited state species on the left side of the reaction.

REFERENCES

EST estimated

EQ calculated from equilibrium and reverse step

BDH72 D.L.Baulch, D.D.Drysdale, D.G.Horne, and A.C.Lloyd, Evaluated Data for High Temperature Reactions, Butterworths, London,1972.

Ba26 J.N.Bardsley, J.Phys.B 1, 365 (1962).

BB72 M.H.Bortner and T.Baurer, ed., Defense Nuclear Agency Reaction Rate Handbook, DNA1948H, 1972.

BGL75 S.W.Benson, D.M.Golden, R.W.Lawrence, R.Shaw, R.W.Woolfolk, EPA Report EPA-600/2-75-019, 1975.

CTC77 D.C.Cartwright, S.Trajmar, A.Chutjian, W.Williams, Phys.Rev.A 16,1041 (1977).

FA72 R.C.Flagan, J.P.Appleton, J.Chem.Phys. 56, 1163 (1972).

Go88 M.F.Golde, Int.J.Chem.Kinetics 20, 75 (1988).

GC68 R.W.F.Gross, N.Cohen, J.Chem.Phys. 48, 2582 (1968).

GR87 G.D.Greenblatt, A.R.Ravishankara, Chem.Phys.Lett. 136, 501 (1987).

GS89 G.Gadd and T.Slanger, to be published.

GT75 K.Glanzer, J.Troe, J.Chem.Phys. 63, 4352 (1975).

HS84 R.K.Hanson, S.Salimian in Combustion Chemistry, W.C.Gardiner, ed., Springer-Verlag, N.Y., 1984, chp. 6.

IB75 M.Imami, W.L.Borst, J.Chem.Phys. 63, 3062 (1975).

Ja86 R.L.Jaffe, Prog.Astro.Aero. 103, 123 (1986).

KBS79 M.Koshi, S.Bando, M.Saito, and T.Asaba, 17th Symp. (Intl.) on Combust., p. 553 (1979).

LH84 M.Y.Louge, R.K.Hanson, Int.J.Chem.Kinetics 16, 231 (1984).

LT74 evaluated from Lewis and Trainor, ARPA report 1092, 1974.

MSS70 J.A.Meyer, D.W.Setser, D.H.Stedman, J.Phys.Chem. 74, 2238 (1970).

Pa85 C.Park, Prog.Astro.Aero. 96, 395 (1985).

Pa87 C.Park, AIAA Paper 87-1574 (1987)

Pa88 C.Park, AIAA Paper 88-0458 (1988)

PCR86 L.G.Piper, L.M.Cowles, W.T.Rawlins, J.Chem.Phys. 83, 3369 (1986).

SAK70 V.H.Shui, J.P.Appleton, J.C.Keck, J.Chem.Phys. 53, 2547 (1970).

SWB73 T.G.Slanger, B.J.Wood, G.Black, J.Photochem. 2, 63 (1973).

TR84 K.Thielen, P.Roth, 20th Symp. (Intl.) on Combust., p. 685 (1984).

WT62 K.L.Wray, J.D.Teare, J.Chem.Phys. 36,2582 (1962).

YB66 R.Young, G.Black, J.Chem.Phys. 44, 3741 (1966).

ZHW76 H. Zacharias, J. B. Halpern, K. H. Welge, Chem.Phys.Lett. 43, 41 (1976).

Zi88 E.Zipf, private communication.

Appendix B

TEMPERATURE DEPENDENT QUENCHING OF THE A $^2\Sigma^+$ AND B $^2\Pi$ STATES OF NO

Temperature dependent quenching of the $A\ ^2\Sigma^+$ and $B\ ^2\Pi$ states of NO

George A. Raiche and David R. Crosley
Molecular Physics Laboratory, SRI International, Menlo Park, California 94025

(Received 20 November 1989; accepted 29 January 1990)

Collisional quenching of the $v' = 0$ vibrational levels of the $A\ ^2\Sigma^+$ and $B\ ^2\Pi$ states of nitric oxide has been studied over the temperature range 300 to 750 K. The pressure dependence of the time decay of laser-induced fluorescence, in a slowly flowing heated cell, furnished the quenching cross sections σ_Q. NO and O_2 quench the A state rapidly but with no temperature dependence; $\sigma_Q = 37$ and 21 Å^2, respectively. σ_{QA} for H_2O drops from 105 Å^2 at 300 K to 34 Å^2 at 750 K. σ_{QB} for O_2 is independent of temperature but σ_{QB} for NO drops twofold and for H_2O decreases by a factor of 3 over the temperature range studied. This variation among these colliders cannot be explained by a uniform, simple picture of the collision dynamics. Evidence is seen for $B \rightarrow A$ transfer proceeding through an intermediate state, perhaps $a\ ^4\Pi$.

INTRODUCTION

The velocity or temperature of a collisional cross section contains important information about the nature of the potential surface on which that collision takes place. If the process is governed by attractive forces, then the cross section will drop with increasing collision velocity or with increased temperature. If it involves repulsive forces or a barrier, then the cross section will become larger as the temperature is increased.

In many cases of electronically excited states of small molecules, cross sections for collisional energy transfer or quenching (i.e., removal of the electronic state) are large, suggesting that attractive forces play a role in those collisions. If so, one would expect those cross sections to drop as the temperature is increased. Quenching of excited states of diatomic hydrides (OH, NH, PH, and CH) has been studied in our laboratory and elsewhere, with varying results.[1] For OH, quenching cross sections drop with increasing temperature for all colliders investigated, so a simple picture of attractive forces appears to hold for this molecule. For the other hydrides, matters are more complex. NH and PH show cross sections decreasing with increasing temperature for some colliders, but not all; for CH, although the cross sections are a few Å^2, they increase with increasing temperature for the four colliders for which comparisons can be made.

This temperature dependence has seldom been investigated for other diatomic molecules. The NO molecule is a good candidate for such study. Its two lowest excited doublet states are the $A\ ^2\Sigma^+$ Rydberg and $B\ ^2\Pi$ valence states, shown in Fig. 1. Cross sections for quenching of the $v' = 0$ level of the A state by the atmospheric molecules O_2 and H_2O, and by NO itself, are known to be at large room temperature: 22, 100, and 38 Å^2, respectively. Similarly large values hold for quenching of the $v' = 0$ level of the B state. Thus long range, attractive forces would appear to play a role in these quenching processes, and a decrease in these cross sections with increasing temperature would be expected.

The temperature dependence of quenching of electronically excited NO has important practical implications as well. NO is particularly suitable for the use of laser-induced fluorescence (LIF) flowfield diagnostics, in part because it is stable over a fairly wide temperature range. It has been used for wind tunnel pointwise measurements[2] and planar imaging in flames and shock tubes.[3] Nonequilibrium gamma band ($A \rightarrow X$) emission has been observed from NO in highly shock heated air.[4,5] Knowledge of the quenching cross section as a function of temperature for a variety of colliders is necessary to derive quantum yields for reduction of the LIF or emission intensities to concentrations. In addition, these collision rates are needed for an understanding of the formation mechanism of radiating excited states in the shock heated air.[6]

In this paper, we describe quenching measurements made on the $v' = 0$ levels of the $A\ ^2\Sigma^+$ and $B\ ^2\Pi$ states of NO, for the atmospherically important colliders N_2, O_2, NO, and H_2O. Quenching is measured for several temperatures between 300 and 750 K. Cross sections for all collision partners but N_2 (and He) are large. However, only for NO quenching of the B state, and for H_2O quenching of both states, is a temperature dependence seen. In all three cases the cross sections decrease with increasing temperature. It thus appears that a consistent interpretation of the energy transfer mechanism, in terms of attractive forces governing all NO collisions that have large quenching cross sections, is not applicable here.

EXPERIMENTAL DETAILS AND RESULTS

The quenching cross sections were measured by monitoring the temporal evolution of the population of each state, following pulsed laser excitation, as a function of quenching gas pressure. The apparatus used in the experiments is straightforward. Nitric oxide, diluted in helium, was mixed with the quencher, also diluted in helium, and the mixture flowed slowly through a glass cell. The sample was heated electrically, using clamshell heaters surrounding the cylindrical cell. The partial pressure of quencher was obtained from the total pressure, measured with a

 0021-9606/90/095211-07$03.00

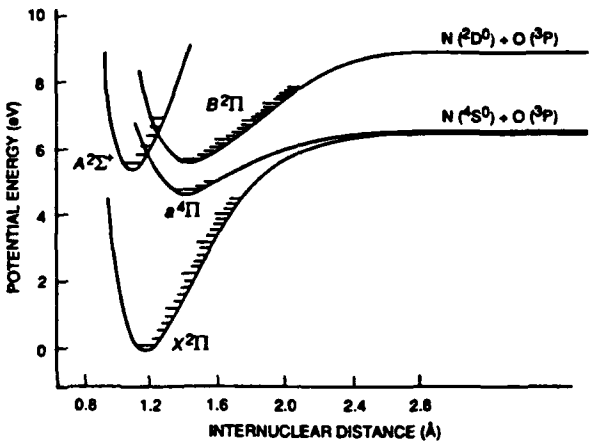

FIG. 1. Potential curves for the states of NO relevant to this study.

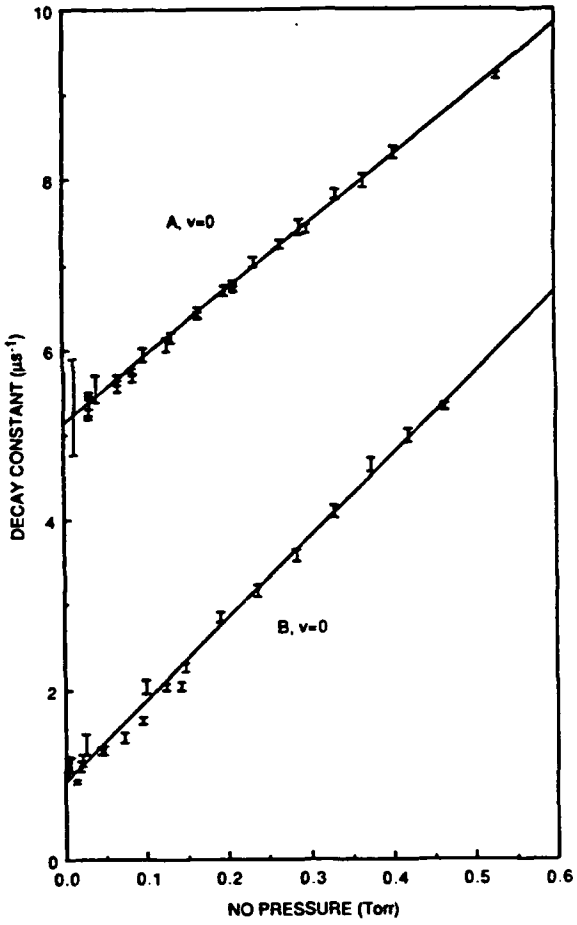

FIG. 2. Plots of decay constant vs pressure of NO at room temperature, for the $A\,^2\Sigma^+$ and $B\,^2\Pi$ states. The rate constant is obtained from the slope of the line, while the intercept represents the radiative rate plus any quenching due to background He.

Baratron gauge, and relative flow rates as measured by mass flowmeters. Special care was taken to determine the water partial pressure. Helium was bubbled through thermostated liquid water, and the relative humidity of the mixture was determined by a capacitance hygrometer humidity indicator on the high pressure side of the flow valve. The partial pressure of H_2O can be determined knowing the vapor pressure. Measurements made over various periods of time ensured that adsorption/desorption processes on the cell walls had reached steady state.

In both the A and B states, a single rotational level in the $v' = 0$ vibrational level was pumped using a tunable dye laser. The laser was an excimer pumped dye laser with pulse length of ~ 10 ns. The A state was pumped via two-photon absorption in the (0,0) band near 453 nm. The B state was excited using one-photon transitions near the 219.9 nm (0,0) origin. Using a beam splitter, fluorescence at right angles was monitored with both a filtered photomultiplier tube and through a monochromator tuned to an appropriate emission feature. In the case of the A state, the γ-band emission extended over the 226 to 300 nm wavelength region. The Franck–Condon factors for the diagonal β-band transitions from the B state are very small; thus, most of this emission, to high v'', is spread over a wide spectral region commencing near 300 nm. For the quenching measurements, specific bands were isolated using the monochromator. The output from the photomultipliers was captured by a transient digitizer to determine the fluorescence decay times. Measurements for quenching of the A state made using the monochromator and by the filtered photomultiplier agreed well; the monochromator was needed for the B-state quenching studies, however, because of interference from $B \rightarrow A$ transfer (see below)

The resistance heaters do not produce a uniform temperature throughout the cell, so that the temperature must be measured at the same point where the fluorescence decays are monitored. For this purpose, rotational temperatures were determined from two-photon excitation scans in the A–X system. (A thermocouple inside the cell is unsuitable because of the large radiant output of the heaters.) Two-photon line strengths were calculated from available formulas[7]; the less congested S branch was most often used although some R- and P-branch lines were also included. The typical statistical uncertainty in the resulting Boltzmann plots was ± 30 K. Checks were performed at intermediate temperatures to determine that we were not saturating the rotational transitions, which would have caused systematic errors in the rotational temperature.

The time resolved traces for A state decay are single exponentials over a large range of pressures. In each case the decay constant at a given pressure is taken from a linear least squares fit of the logarithm of the signal vs time, from 90% to 10% amplitude. The B state decay is not strictly exponential at low pressures, probably due to rotationally mediated energy transfer as discussed below. However, at higher pressure it can be fit to a single exponential to determine the decay constants. Plots of decay constant vs collider pressure then yield the quenching rate constants. Examples for NO self-quenching of the A and B state are shown in Fig. 2, and for H_2O quenching of the A state at different temperatures in Fig. 3.

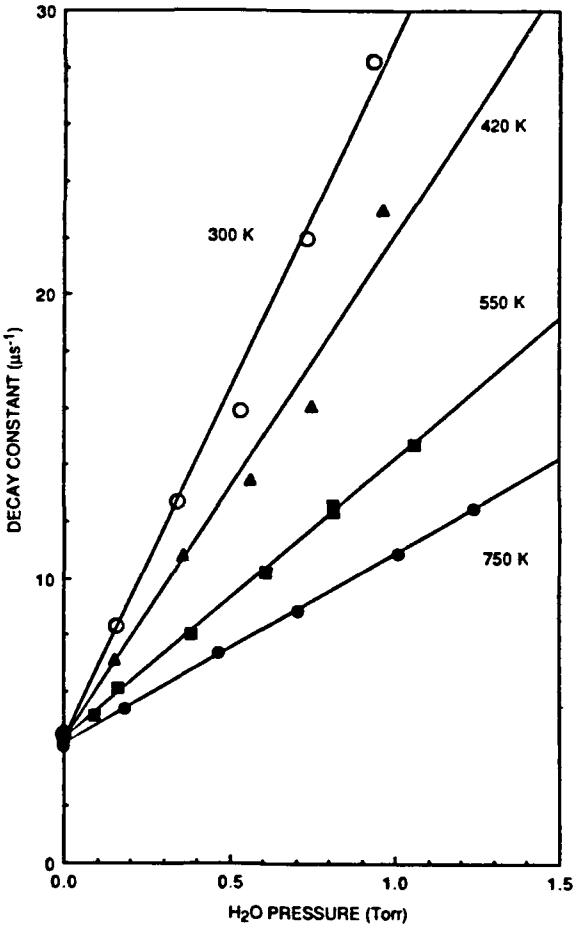

FIG. 3. A-state decay constant plots vs pressure for H_2O collider at four different temperatures. For a constant cross section, the slopes would decrease as $T^{-1/2}$. They fall faster, indicating that the cross section itself decreases with increasing T.

Error bars calculated for the cross sections of water quenching are considered as the upper bounds for the uncertainties of all cross sections. The major contributions to the error bars are the statistical uncertainties in the rate constants taken from the slope of decay constant vs pressure plots, and in the LIF temperatures taken from the slope of Boltzmann plots. For quenching of the NO B state by H_2O, statistical uncertainties in the worst cases approach 30% of the rate constant. However, the majority of the rate constants and temperatures for other quenchers are determined (statistically) to better than 10%, which is the basis of our error bars.

The zero pressure intercepts of the plots in Figs. 2 and 3 correspond to the radiative lifetime, plus any quenching due to the background helium carrier gas. In the case of the A state, that residual quenching contributes a negligible amount, and the measured intercepts agree well with the well established $\tau_{rad}(A)$ of 220 ns. In the case of the B state, the τ_{rad} is a matter of current dispute. Although the currently accepted value is near 3 μs, recent measurements[8] indicate the correct value should be 1.5 to 2 μs for the $v' = 0$ level of $B\,^2\Pi$. In our measurements there exists some residual quenching due to the He carrier (Fig. 2), and our results are essentially in agreement with the values of Ref. 8.

The quenching rate constants contain an uninteresting temperature dependence through the average collision velocity $\langle v \rangle = \sqrt{8kT/\pi\mu}$. Thus we convert the results to thermally averaged cross sections, by dividing the experimental rate constants by $\langle v \rangle$. Results are listed in Table I. Errors in the quenching cross sections are compounded of statistical errors as computed from the fitting procedure and uncertainties in the quencher partial pressures and temperature. Fluctuations in the total gas flow rate, induced by changes in the flow rates of added collider, could affect individual decay constant measurements by changing the background pressure of NO. In order to prevent this, it was necessary, for some colliders, to adjust all the gas flows to keep the total flow constant. This was needed for colliders of small cross section, i.e., N_2 and He, where large partial

TABLE I. NO quenching cross sections, Å^2.

	A state				
Temperature	300 K	420 K	550 K	725 K	750 K
NO	37±3	···	35±4	···	37±4
O_2	21±3	···	21±4	···	19±4
N_2	<0.01	···	···	···	<0.1
H_2O	106±10	84±5	55±4	43±4	34±3

	B state					
Temperature	300 K	500 K	550 K	600 K	725 K	750 K
NO	43±3	···	21±3	···	22±3	···
O_2	2.9±0.3	2.3±0.5	···	2.5±0.5	3.2±0.6	···
N_2	0.071±0.005	···	···	···	···	···
H_2O	17±2	6.8±2.1	···	6.0±0.7	···	4.8±1.2
He	0.030±0.003	···	···	···	···	···

TABLE II. $A\,^2\Sigma^+$, $v' = 0$ quenching cross sections at 300 K, Å^2.

	This study	Ref. 9	Ref. 10	Ref. 11	Ref. 12	Ref. 13
NO	37±3	···	41±6	···	40	···
O_2	21±3	22±1	23±4	22±2	29	36±5
N_2	<0.01	0.014±0.004	<0.015	···	<0.01	···
H_2O	106±10	101±9	104±14	···	···	97±10

pressures were required to observe any quenching. The same was true for H_2O since, although the cross sections are large, the effective concentration of H_2O in its helium-diluted flow is less than 1%.

QUENCHING OF THE *A* AND *B* STATES

Comparison with other room temperature measurements

We begin our examination of the results in Table I by a comparison with other measurements made at room temperature. Quenching of the $A\,^2\Sigma^+$ state of NO has been studied extensively, although we will consider only five investigations.[9–13] In two recent measurements,[9,10] the pressure dependence of time decay of LIF was used, as in the present work. Table II displays the results from those studies for the four colliders studied here; the agreement is excellent in all cases.

Quenching of the *A* state has also been investigated by Stern–Volmer intensity measurements as a function of added collider pressure. The procedure yields the quenching rate constant in units of radiative rate; an independent value of the radiative lifetime is needed to determine the quenching rate constant. In Refs. 11 and 12, the excitation source was a tunable laser. In Ref. 13, the γ-band emission was chemiluminescence in a discharge in NO. The results listed for Ref. 13 in the last column of Table II have been corrected to correspond to the proper lifetime of 220 ns for the *A* state. Even though Stern–Volmer analyses can be subject to systematic errors, especially in discharges, the agreement here is also quite good.

Low vibrational levels of the *B* state have been little studied, compared with the *A* state, due largely to the low band transition probability for direct excitation from $v'' = 0$ of the ground state. All three prior studies determined quenching rates via Stern–Volmer intensity plots of emission from $B\,^2\Pi$ produced three different ways: in a discharge,[13] by NO_2 photodissociation,[14] and by energy transfer[15] from $A\,^2\Sigma^+$ NO selectively excited in a cell. A compilation of these results and the present ones is given in Table III. In each case, the reported rate constants have been adjusted to correspond to the recently measured radiative lifetime of 2.0 μs for the $v' = 0$ level.[8] Here we see much poorer agreement than was the case for the single-level excitation experiments for the *A* state in Table II; most of the *B* state cross sections differ by factors of 2 to 10. This situation is not considered unreasonable in comparing cross sections derived from intensity measurements such as those in Refs. 13–15. We do note that our result for O_2 is conspicuously lower than those measured earlier, but have no explanation for this difference.

Temperature dependent cross sections

The large cross sections for several of the colliders studied, O_2, NO, and H_2O for $A\,^2\Sigma^+$, and NO and H_2O for $B\,^2\Pi$, suggest that long range, attractive forces play a role in the quenching of these electronically excited states of nitric oxide. A process governed by a purely attractive surface should have a cross section which decreases with increasing temperature (i.e., collision velocity). However, the temperature dependence of NO quenching is varied, as shown by the results in Table I. For the *A* state, quenching cross sections for NO and O_2 do not vary with temperature, whereas that for H_2O decreases by about a factor of 3 over the temperature range covered, 300 to 750 K. This is illustrated in the plot of Fig. 4. For the *B* state, quenching by NO and H_2O drops with increasing temperature, by a factor of 2 and 3, respectively; see also Fig. 4. That for O_2 is constant, although the smaller size of the cross section, 3 Å^2, indicates that here repulsive forces may play a role or even dominate.

Quenching by O_2 was examined at two different temperatures in the chemiluminescent discharge experiments.[13] For the *A* state, the cross sections were 21±4 Å at 298 K and 34±5 Å^2 at 195 K; we have used the authors' fractional error bars, which appear to be derived from the scatter in the Stern–Volmer plots. Thus there is some indication of a temperature dependence, in contradiction to our results, although the variation is not much outside the combined uncertainties. The *B* state was also studied at these same two temperatures, with the results of 38±5 Å^2 at 298 K and 47±6 Å^2 at 195 K. There is here the same indication although these error bars overlap. On the other hand, the large difference between this cross section and our value of 3 Å^2 at 300 K precludes a meaningful comparison of the temperature dependence.

TABLE III. $B\,^2\Pi$, $v' = 0$ quenching cross sections at 300 K, Å^2.

	This study	Ref. 13	Ref. 14	Ref. 15
NO	43±3	···	···	20±1
O_2	2.9±0.3	21±4	37±7	···
N_2	0.071±0.005	···	0.14±0.03	···
H_2O	17±2	50±13	···	···
He	0.030±0.003	···	0.03±0.01	···

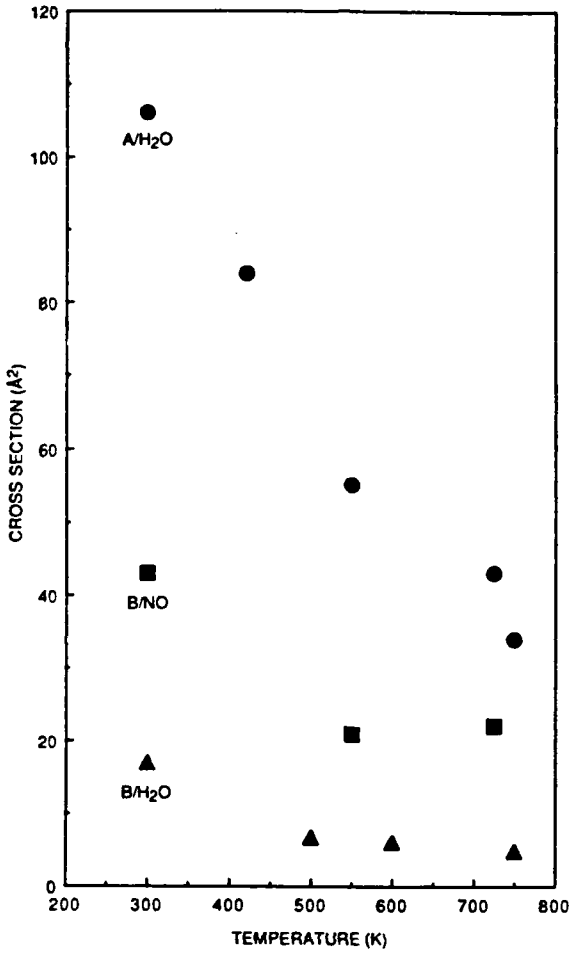

FIG. 4. The three temperature-dependent cross sections plotted against temperature to illustrate the magnitude of the decrease. Circles: $\sigma_{Q4}(H_2O)$; squares: $\sigma_{QB}(H_2O)$; triangles, $\sigma_{QB}(NO)$.

Quenching of the A state by H_2O at higher temperatures has been measured recently.[16] Hydrogen/oxygen/argon flames seeded with NO were burned at low pressure; because the three body recombination reactions are slow at reduced pressure, the temperature in the burnt gases can be well below the adiabatic flame temperature.[17] In this flame at temperatures near 1200 K, the predominant quencher is probably H_2O, although there may also be contributions from H atoms, which are known to quench OH rapidly at these temperatures.[18] The decay rates measured in flames at 19, 38, and 76 Torr were converted to cross sections, assuming all the quenching was due to H_2O. The result was a cross section 35 ± 3 Å^2 at 1340 K, and the same (within error bars) at 1150 and 1020 K.

The cross section measured in the flame between 1000 and 1340 K is the same 35 Å^2 as at the upper end of our temperature range, 750 K. A decrease in the rate of change or even a leveling off of the cross section at higher temperature remains consistent with a collision governed by attractive forces. Such behavior has also been observed for the quenching of $A\,^2\Sigma^+$ OH radicals over a wide temperature range for the polar colliders ammonia[19] and water,[18] where attractive forces are known to play a role.[1]

Models for NO quenching collisions

A suitable interpretation of the quenching mechanism must explain all facets of the experimental results: the variation in cross section among different colliders, the overall size of the cross sections, and the varied temperature dependence. We note here there are several different models, all involving attractive forces, which have been advanced to explain electronic quenching of various small molecules. None is capable of explaining all the experimental observations on NO.

Three parametric correlations have been offered by Thayer and Yardley,[20] Selwyn and Steinfeld,[21] and Parmenter and co-workers.[22] The Thayer–Yardley picture, which has been explicitly examined[11] for NO quenched by a number of colliders, contains a weak $T^{-1/5}$ temperature dependence of the cross section. The Selwyn–Steinfeld model predicts $\sigma \sim T^{-1/2}$, and the Parmenter correlation $\sigma \sim \exp(a/T)$. None of these satisfactorily explains the variation in cross sections with collider, nor the differing temperature dependences found here.

A model[23] based on a multipole interactions between the radical and the collider has been generally successful for OH, although not[1] for CH and NH. NO is weakly polar in both the A (Ref. 24) and B(Ref. 25) excited states, with dipole moments $\sim$0.2 D. However, it should be highly polarizable, so that $1/R^6$ dipole-induced dipole and/or dispersion forces might be expected to dominate the long-range interactions even for polar colliders. This interaction would lead to a $T^{-1/3}$ temperature dependence for all colliders, again inadequate. It also cannot explain the very small cross sections observed for N_2 collider.

A different model has been suggested by Ascher and Haas[11,12] to describe their results on quenching of several vibrational levels of NO $A\,^2\Sigma^+$. This picture is a "harpoon" electron transfer mechanism in which NO and the collision partner switch from covalent to ion-pair curves at some crossing radius. Qualitative agreement is achieved for many colliders, certainly as good as that for any of the other models. Especially appealing is the prediction[11] of a zero cross section for N_2 due to the absence of a curve crossing; the same phenomenon also explains small cross sections[12] for CF_4, CH_4, and SiF_4. An explicit temperature dependence cannot be extracted from the treatment given in Refs. 11 and 12, but the nature of the interactions involved again demands a decrease in the cross section with increasing temperature for all colliders. As for all the other models, this is at variance with the experimental results.

ENERGY TRANSFER FROM B TO A

$A\,^2\Sigma^+$ emission can be observed following excitation of the $B\,^2\Pi$ state. We describe here the preliminary observations both on dual exponential decay of B and this transfer of excitation, which are consistent with the participation of a third electronic state.

For the A state, individual plots of signal vs time are single exponentials over a range of pressures, and the zero-pressure intercepts of plots such as Figs. 2 and 3 correspond to accepted values of the radiative rate. For the B

state, however, double exponential decay becomes apparent at lower pressures (<500 mTorr) of collider gas. A faster initial component is followed by a slower decay. At higher pressures, the decay curves are again well fit by a single exponential (our reported cross sections, Table I, are derived from fits under these conditions). This behavior was also observed for the $v'=3$ vibrational level the $B\,^2\Pi$ valence state of the NS molecule[26] where it was attributed to mixing with a quartet state. It can be interpreted in terms of the familiar "gateway" model, in which only particular rotational levels are perturbed and cause state mixing. First, rapid collisional rotational transfer occurs to the perturbed level in B which is coupled to the long-lived quartet. Rotational redistribution within the quartet then takes place; some of the population leaks back into B which then radiates. The slower second exponential represents this repopulation of the emitting B state. At higher pressures, rotational equilibrium in the quartet and the transfer back into B both occur very rapidly and only a single component is observed, caused by collisional removal of the pair of states.

A prime candidate for the coupled state is the elusive $a\,^4\Pi$ state, which is known[27] to perturb both A and B, and has been invoked to explain a variety of photophysical phenomena in the A, B, and C states of NO (see Ref. 28 for a discussion). The B, $v'=0$ state is located near $a\,^4\Pi$, $v'=8$; and the A, $v'=0$ state is near $a\,^4\Pi$, $v'=6$. The A state, while imbedded in the quartet as is B, shows only single exponential decay for all pressures. This is because the faster radiative rate (ten times that of B) dominates the overall A-state removal process at moderate collider pressures, when the redistribution within the quartet is occurring. At higher pressures, where collisions do contribute significantly to the total removal rate, this equilibration and back transfer is completed rapidly.

Using the monochromator, γ band A–X emission could be observed following excitation of the B state under collisional conditions. Figure 5 shows representative spectra. Here the B state has been pumped and can be observed through the (0,4) band near 262 nm while the $v'=0$ level of the A state, populated by energy transfer, emits in the (0,3) band near 259 nm. Note that the Einstein A coefficient[29] for the (0,4) β band shown is some 80 times smaller than that for the (0,3) γ band, so that only a small fraction of the B state decay is transferring into A. As the pressure of NO is increased, the A–X band intensity grows in relative to the B–X band. From time and wavelength resolved studies, we estimate that between 2% and 3% of the B state population, quenched by NO itself, is transferred into the A state. This phenomenon is also seen, although with less transfer, for N_2 and O_2 colliders.

Time resolved traces can be captured with the transient digitizer, tuning the monochromator to look at emission from only one electronic state. Figure 6 shows such traces for 500 mTorr of NO at room temperature. In the top trace, for reference, is an A–X decay curve obtained by directly pumping the A state. In the middle panel is the B–X decay obtained directly pumping B. Its decay is collision dominated under these conditions, in contrast to A which decays mainly radiatively. In the bottom trace is A–X emission following pumping of the B state. Its time dependence may be described by the sum of two exponentials, the slower one the decay of the B state and the faster the decay of A (note that the population in A always increases at the faster rate regardless of its physical interpretation).

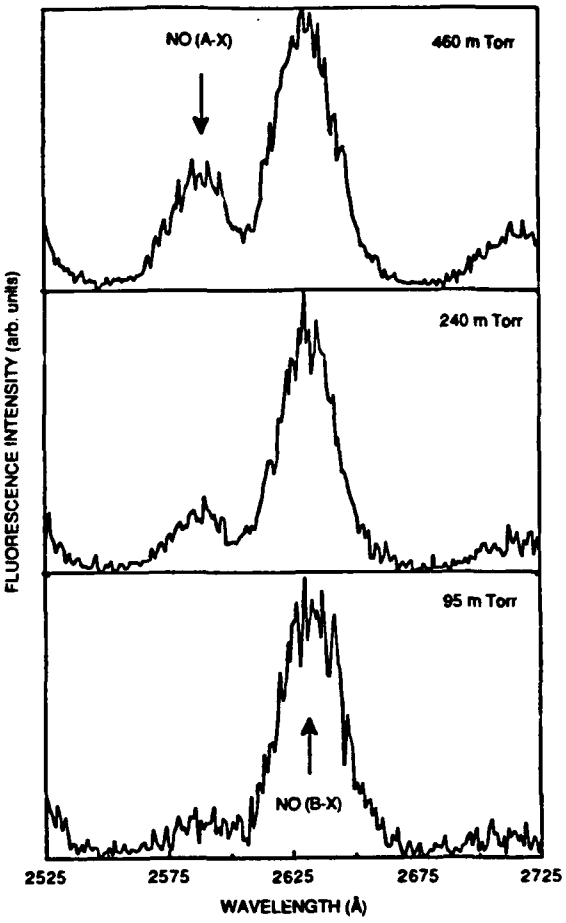

FIG. 5. Fluorescence spectra, time integrated over the entire fluorescence decay, following excitation of $B\,^2\Pi$, at three different NO collider pressures. Shown are the B–X (0,4) band and the A–X (0,3) band. As the pressure increases, the A–X emission intensity grows in relative to B–X.

Decay constants can be obtained from traces such as those at the bottom of Fig. 6 and plotted vs pressure to obtain collision cross sections. We expected the pressure dependences to correspond to those measured earlier, using the decay from each state when it is directly excited, but they do not. Both sets of decay constants have the same pressure dependence. Therefore, the observations illustrated in Fig. 6 do not correspond to transfer directly from B to A. Rather, we interpret these results in terms of the metastable $a\,^4\Pi$ state, which is filled from B and then decays into A. As noted above, this same interpretation can also account for the nonexponential decay of B at low collider pressures. A more extensive study of this interesting $B \rightarrow A$ electronic-to-electronic state transfer, apparently mediated by the elusive $a\,^4\Pi$ state of NO, is clearly warranted.

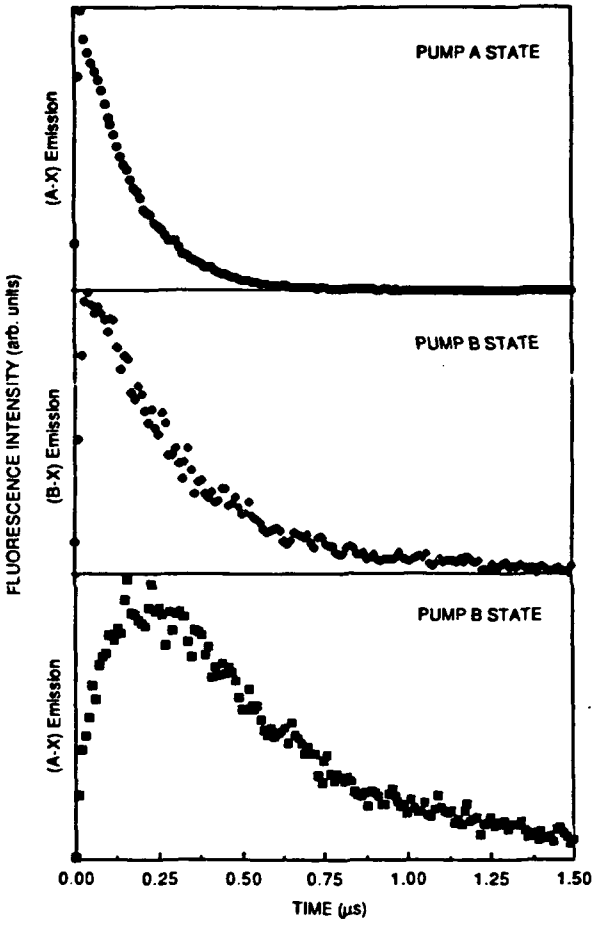

FIG. 6. Time-resolved fluorescence traces with NO as the collider at a pressure of 250 mTorr. Top: Single-exponential A-state decay following direct excitation of $A\,^2\Sigma^+$. Middle: Single-exponential B-state decay following direct $B\,^2\Pi$ excitation. Bottom: A-state decay following excitation of $B\,^2\Pi$.

CONCLUSION

Quenching of NO $A\,^2\Sigma^+$ and $B\,^2\Pi$ has been studied for several colliders over the temperature range 300 to 750 K. The temperature dependence is varied, even for colliders with large cross sections. Although attractive force interactions are indicated, a simple interpretation in terms of a single mechanism applicable to all colliders is not possible. Instead, matters appear more interesting and need separate examination for each collider. The B and A states are quenched with very similar efficiencies by NO itself; why temperature dependences are different may provide important insights. The dual exponential decay of the B state and preliminary results on B to A transfer are consistent with mediation by another electronic state, for which $a\,^4\Pi$ is a prime candidate.

ACKNOWLEDGMENTS

We thank Gregory P. Smith, Jay B. Jeffries, and Tom G. Slanger for useful discussions, and Michael L. Wise for help taking some of the data. This work was supported by SDIO/IST under a contract managed through the U. S. Army Research Office.

[1] D. R. Crosley, J. Phys. Chem. 93, 6273 (1989).
[2] R. L. McKenzie and K. P. Gross, Appl. Opt. 20, 2153 (1981).
[3] B. K. McMillin, M. P. Lee, P. H. Paul, and R. K. Hanson, AIAA Paper 89-2566, Joint Propulsion Conference, Monterey, California, July 1989.
[4] R. A. Allen, P. H. Rose, and J. C. Camm, AVCO Everett Research Laboratory Report No. 156, 1962.
[5] W. H. Wurster, C. E. Treanor, and M. J. Williams, AIAA Paper 89-1918, Fluid Dynamics, Plasma Dynamics, and Lasers Conference, Buffalo, New York, June 1989.
[6] G. P. Smith, D. R. Crosley, and D. J. Eckstrom, SRI International Report MP 89-037, 1989.
[7] J. B. Halpern, H. Zacharias, and R. Wallenstein, J. Mol. Spectrsc. 79, 1 (1980).
[8] G. E. Gadd and T. G Slanger, J. Chem. Phys. 92, 2194 (1990).
[9] I. S. McDermid and J. B. Laudenslager, J. Quant. Spectrosc. Radiat. Transfer 27, 483 (1982).
[10] G. D. Greenblatt and A. R. Ravishankara, Chem. Phys. Lett. 136, 501 (1987).
[11] M. Asscher and Y. Haas, J. Chem. Phys. 76, 2115 (1982).
[12] Y. Haas and G. D. Greenblatt, J. Phys. Chem. 90, 513 (1986).
[13] I. M. Campbell and R. S. Mason, J. Photochem. 8, 321 (1978).
[14] G. Black, R. L. Sharpless, and T. G. Slanger, J. Photochem. 5, 435 (1976).
[15] L. A. Melton and W. Klemperer, J. Chem. Phys. 59, 1099 (1973).
[16] R. J. Cattolica, T. G. Mataga, and J. A. Cavolowsky, J. Quant. Spectrosc. Radiat. Transfer 42, 499 (1989).
[17] K. Kohse-Höinghaus, J. B. Jeffries, R. A. Copeland, G. P. Smith, and D. R. Crosely, Twenty-Second Symposium (International) on Combustion, The Combustion Institute, Pittsburgh, 1988, p. 1857.
[18] J. B. Jeffries, K. Kohse-Höinghaus, G. P. Smith, R. A. Copeland, and D. R. Crosley, Chem. Phys. Lett. 152, 160 (1988).
[19] J. B. Jeffries, R. A. Copeland, and D. R. Crosley, J. Chem. Phys. 85, 1898 (1986).
[20] C. A. Thayer and J. T. Yardley, J. Chem. Phys. 57, 3992 (1972).
[21] J. E. Selwyn and J. I. Steinfeld, Chem. Phys. Lett. 4, 217 (1969).
[22] H. M. Lin, M. Seaver, K. Y. Tang, A. E. W. Knight, and C. S. Parmenter, J. Chem. Phys. 70, 5442 (1979); C. S. Parmenter and M. Seaver, Chem. Phys. Lett. 67, 279 (1979).
[23] D. L. Holtermann, E. K. C. Lee, and R. Nanes, J. Chem. Phys. 77, 5327 (1982); P. W. Fairchild, G. P. Smith, and D. R. Crosley, *ibid.* 79, 1795 (1983).
[24] S. R. Langhoff, C. W. Bauschlicher, Jr., and H. Partridge, J. Chem. Phys. 89, 4909 (1989).
[25] S. R. Langhoff (private communication, 1989).
[26] I. J. Wysong, J. B. Jeffries, and D. R. Crosley, J. Chem. Phys. 91, 5343 (1989).
[27] E. Miescher, J. Chem. Phys. 73, 3088 (1980).
[28] T. G. Slanger, in *Reactions of Small Transient Species*, edited by A. Fontijn and M. A. A. Clyne, (Academic, London, 1983), p. 231.
[29] M. L. Wise, G. A. Raiche, and D. R. Crosley (to be published).

Appendix C

LASER-INDUCED FLUORESCENCE DECAY LIFETIMES OF SHOCK-HEATED NO ($A^2\Sigma^+$)

Appl. Phys. B 53, 138–141 (1991)

Applied Physics B Photophysics and Laser Chemistry

Laser-Induced Fluorescence Decay Lifetimes of Shock-Heated NO ($A^2\Sigma^+$)

U. E. Meier*, G. A. Raiche, D. R. Crosley, G. P. Smith, and D. J. Eckstrom**

Molecular Physics Laboratory, SRI International, Menlo Park, CA 94025, USA

Received 16 May 1991/Accepted 25 June 1991

Abstract. Radiative emission in the NO γ-band system occurs when air at a few Torr initial pressure is shock-heated at sufficiently high temperatures of 3500–7000 K. Emission spectra of this system in shocks indicate that collisional quenching of the emitting $A^2\Sigma^+$ state is a critical quantity controlling the intensity. Quenching of excited NO by NO itself has been measured using direct time decay of laser-induced fluorescence in the shock tube at 3500 K. The cross section ($2-\sigma$ error) is 59 ± 20 Å^2, compared to the room temperature value 37 ± 8 Å^2. At 3500 K, N_2 also quenches NO with a cross section ~ 2 Å^2, much larger than the value at 300 K.

PACS: 34.50Gb

In reactive flows at high velocity and low pressure, the time scales for energy transfer and chemical reaction become comparable to the flow times themselves. This can result in nonequilibrium chemical compositions and nonequilibrium vibrational and electronic state populations, with significant effects. Among these are the characteristics of the external flowfield upon re-entry of the space shuttle and aerospace planes, heat transfer to surfaces, and the hydrogen/air combustion chemistry of the spaceplane's scramjet propulsion system. Of interest also is the observable ultraviolet emission found in air heated by bow shock waves, whose maximum intensity occurs in regions of nonequilibrium chemistry and energy transfer.

We have investigated the spectral emission in the γ-band system of nitric oxide in shock-heated air, and the decay lifetimes of the emitting $A^2\Sigma^+$ state. The experiments are directly connected to the observation of γ-band emission in the bowshocks of ascending rockets in the 40–70 km range [1]. These altitudes correspond to preshock pressures between 5 and 0.1 Torr, and the rocket speeds are typically 3.5 km/s.

The mechanisms by which the excited state of NO is populated are not at all well established. The nonequilibrium chemistry which forms the ground state NO from hot air, and possible routes for exciting the molecule to the $A^2\Sigma^+$ state, are discussed in [2]. These routes include energy transfer from metastable $A^3\Sigma_u^+$ N_2, recombination of N and O atoms, electron impact excitation, and heavy particle excitation directly from the ground state. The last of these possibilities, together with an estimated generic excited state removal (quenching) cross section of 1 Å^2, is a major source considered in a computer model of the bowshock chemistry and radiation [3] designed for re-entry questions. Adapted to the problem of ascent bowshocks [4], it predicts a much sharper drop in emission intensity with increasing altitude (decreasing density) than was observed in the flight experiment [1].

Our shock tube measurements are of two types. The first, the observation of the emitting γ-band system in the shocks, indicated that collisional quenching plays a critical role in determining the total γ-band radiance, and must account for a significant part of the removal of the excited state. This led to the second set of measurements, the determination of high temperature collisional quenching cross sections σ_Q for the emitting $A^2\Sigma^+$ of NO. This was done through measurement of the direct time decay of laser-induced fluorescence (LIF) of NO in NO/buffer gas mixtures shock-heated to 3500 K. Because σ_Q varies with temperature for some but not all colliders [5], it is necessary to perform these experiments directly at high temperature. The results on NO self-quenching indicate a slight increase in σ_Q from its room temperature value. N_2 also appears to be a significant quencher of NO at high temperature, in contrast to its negligible role at 300 K. In addition to this role in the problem of shock-heated air, the understanding of quenching of electronically excited

* Sabbatical visitor, on leave from DLR Stuttgart, Fed. Rep. Germany

** Present address: Department of Chemistry, Hamilton College, Clinton, NY 13323, USA

NO is also important for interpreting experiments designed to probe NO with LIF, as has been done in shock tubes [6] and in flames [7, 8].

1. Emission Spectra Measurements

The stainless steel shock tube used for these experiments has a 5 cm internal diameter and is 4.6 m long with a 1.3 m driver section. It was operated with room temperature helium or, usually, hydrogen driver gas to produce shock velocities up to 4.5 km/s at an initial test pressure of 0.5 Torr, corresponding to an altitude of 50 km. Initial pressures ranging upwards from this value to 2 Torr were used. The experiments were conducted in the incident shock mode. The radiative emission from the incident shock, apertured at the observation window 35 mm from the end of the tube with a 2 mm slit, was imaged onto a spectrometer and detected with an enhanced, intensified linear array (Princeton Instruments). A detection gate of typically 2.5 μs duration was triggered immediately upon arrival of the shock wave at the detection plane, as measured by a piezoelectric transducer. A laser schlieren arrangement was used to ensure that the transducer correctly determined the arrival time.

Measurements were made of the emission from NO formed directly in the shock heated air. The chemical reactions for this process [2] involve, sequentially, dissociation of O_2 and reaction of the O atoms with N_2, followed by reaction of N atoms with O_2. Emission measurements were also made in which NO, at concentrations $< 5\%$, was seeded into other pure gases: N_2, O_2, N_2O, CO_2 and Ar, and in neat NO. The shock speeds were about 4.4 km/s, corresponding to initial temperatures near 9500 K and a final temperature close to 4600 K for all mixtures except Ar, N_2 and CO_2, where $T_{eq} \sim 6000$ K at the observation times used (integration of a shock tube kinetics code [9] was used to determine these temperatures).

A typical spectrum in synthetic air is shown in Fig. 1. Those in N_2, Ar, NO, and N_2O all appeared similar, all showing several vibrational bands in the $v' = 0$, 1 and 2 progressions of the γ-system between 200 and 300 nm, with comparable intensities in each progression. They agree reasonably well with those observed in other shock tube experiments [10] and in the rocket flight tests [1]. Unfortunately, our available detection gate and spatial resolution do not provide sufficient time resolution to capture the emission only in the interesting nonequilibrium regime. (This is also true for the other shock tube experiments [10].) Therefore our initial objective of using measurements of the nascent vibrational distribution in air to discern the mechanism for populating $A^2\Sigma^+$ NO was not attained with this experimental configuration.

However, the intensity of the γ-band emission in different mixtures was revealing. In contrast to the spectra observed in neat NO mixtures in air, N_2, Ar, and N_2O, no emission was found for NO seeded into O_2 and CO_2. Because the NO $A^2\Sigma^+$ must be formed as well here as in the other mixtures, these results indicate efficient collisional removal of the excited state by O_2 and CO_2

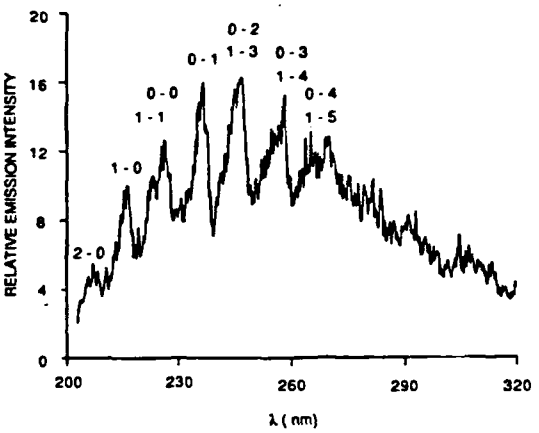

Fig. 1. NO γ-band emission spectrum from a shock in synthetic air (79% N_2, 21% O_2) with speed 4.46 km/s (Mach 12.9) and temperature 4600 K. The cold gas pressure is 0.5 Torr, and the hot gas pressure 100 Torr. The array detector gate was 2.5 μs duration triggered at the shock front arrival time

at these high temperatures. (The final equilibrium temperatures are somewhat cooler in CO_2, because of heat capacity differences, although the initial, nonequilibrium temperature is about the same for all mixtures; note also that the majority gas in the N_2O experiments is N_2, because of chemical reaction.) The overall radiance from NO is inversely proportional to the rate of this collisional removal, so quenching must play a critical role in any description of γ-band emission from shock-heated air. These results suggest that at high temperature there are considerable differences in quenching contributions from different buffer gases. These questions formed the impetus for undertaking the LIF decay measurement of quenching in the shock tube, described in the next section.

2. LIF Time-Resolved Decay Measurements

Although quenching of $A^2\Sigma^+$ NO has been studied for a variety of colliders at room temperature, only recently has the temperature dependence of its quenching been investigated. The cross sections [5] σ_Q for quenching by O_2, H_2O and NO itself are large at room temperature (21, 104 and 37 Å^2, respectively). This immediately suggests the influence of attractive forces and the expectation that σ_Q will decrease with increasing temperature, as for the OH radical [11]. Knowledge of this dependence is obviously crucial when considering processes occurring at the temperatures of shock-heated air.

LIF decay measurements have been performed in a heated cell [5]. These showed that σ_Q fo H_2O decreased from 106 to 34 Å^2 over the range 300-750 K, as anticipated. Measurements in a flame [12] between 1100 and 1300 K agree with these results. Surprisingly, however, σ_Q in the heated cell experiments for both O_2 and NO remained constant over this range. Quenching by N_2 was small, < 0.1 Å^2 at 750 K and $\lesssim 0.01$ Å^2 at 300 K. Extrapolation to the much higher shock temperatures cannot be made given the lack of understanding of the quenching mechanism and the reason for these differing temperature dependences.

Therefore, quenching measurements were performed directly in the shock tube at the appropriate temperatures, using time-resolved LIF. Although we observed time-resolved decays in shock-heated air, the quantitative measurements were performed with NO seeded into other mixtures. We report measurements for quenching by NO itself and by N_2.

The $v' = 0$ level of the $A^2\Sigma^+$ state was excited using a tunable dye laser, frequency doubled to 226 nm wavelength, with pulses of ~ 10 ns duration. A bandhead was chosen to furnish maximum fluorescence intensity; the exact rotational level(s) excited is not important because quenching of $A^2\Sigma^+$ NO does not vary with rotational level [13]. The laser was directed at right angles to the shock propagation direction, and the fluorescence was observed at right angles using the same 2 mm slit as in the emission experiments. Spectral filtering was provided using the monochromator as a bandpass filter, or using a 288 nm interference filter. Detection was by a Hamamatsu R166UH tube, and the signals were collected into a digital storage oscilloscope having a 200 MHz bandwidth.

Measurements were made at two nominal concentrations of NO seeded into 0.5 Torr cold N_2. The lower value was a cold NO pressure of 0.011 Torr, and the higher 0.04 Torr. For these experiments He was used as the driver gas, to produce a shock speed of 2.8 ± 0.1 mm/μs, calculated final temperature between 3450 and 3550 K, and a shocked gas pressure ~ 40 Torr. The decay measurements, one trace for each shock, were performed several μs after passage of the shock front. At this point, thermalization of vibrational populations has occurred; at these temperatures, there is no significant chemical reaction and the gas composition is the same as in the cold preshock gas.

The laser and storage scope are externally triggered by a pulse delayed 0.1 μs from the output of the piezoelectric crystal at the observation position. The excimer pump laser (Lambda Physik EMG50) is concomitantly and continuously fired by its internal trigger at a slow rate to avoid damage from constant high voltage, because the diaphragm burst pressure and time cannot be foretold accurately.

A typical decay trace is shown in Fig. 2. The single shot decay shown here has a lifetime of ~ 100 ns. This trace is fit to a single exponential from 90 to 10% of the maximum amplitude to obtain a decay constant. Measurements were made for five shots at the lower seeding pressure and six at the higher. Temperatures and densities were calculated from the measured cold pressure and shock speed for each shot using the Sandia shock tube code [12]. An estimated 5% uncertainty in shock speed propagates to $< 2\%$ error in final density. Results, in the form of a plot of decay constant vs. NO density, are given in Fig. 3. The slight differences in NO density in each of the two groupings are due to both slightly different cold gas mixtures and different diaphragm burst pressures (hence different temperatures) from shot to shot.

The data shown in Fig. 3 all arise from single shot decay traces as in Fig. 2 and have error bars, determined by the goodness of fit to the single exponential, ranging

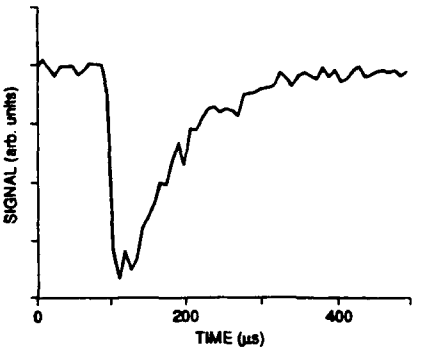

Fig. 2. Single shot laser-induced fluorescence decay trace for NO ($A^2\Sigma^+$, $v' = 0$). Observation is behind the incident shock at a temperature of 3430 K, with postshock pressures of 0.832 Torr NO and 40.7 Torr N_2

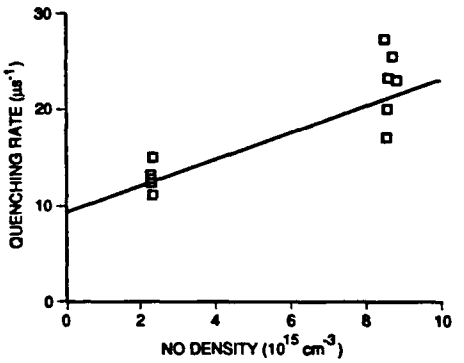

Fig. 3. Decay rate of NO vs. NO density. Each point is the result of a single exponential fit to a decay trace as in Fig. 1; error bars are not shown but range from 5–20%. The slope of the plot yields the quenching rate coefficient. The line drawn is from the unweighted fit; the use of different weightings yields somewhat different rate coefficients as discussed in the text

between 5 and 20%. Consequently the result of fitting the data to a slope vs. density depends upon the weighting function chosen. If the data are unweighted, the slope (which is shown in Fig. 3) corresponds to a rate constant $k_Q = (1.49 \pm 0.27) \times 10^{-9}$ cm^3 s^{-1} for quenching of excited NO by NO. The cross section $\sigma_Q = k_Q/\langle v \rangle$, where $\langle v \rangle$ is the mean relative velocity, is 67 ± 12 Å^2. The error bars are $1-\sigma$ values from the unweighted least-squares fit in Fig. 3; the correlation coefficient for the fit is 0.88.

If, however, the points are weighted in inverse proportion to their error bars, we obtain $\sigma_Q = 59 \pm 10$ Å^2; if the weighting is in inverse proportion to the square of the error bars, the result is $\sigma_Q = 52 \pm 9$ Å^2. Again, these are $1-\sigma$ errors; the correlation coefficient is the same. This dependence of numerical result upon fitting procedure is largely a comment on the scatter of the data (Fig. 3) and suggests that no one weighting method is definitive. We adopt the middle value of 59 Å^2 as a reasonable compromise.

Bearing in mind the dependence of the result on the weighting, we can compare the cross section at 3500 K with the low temperature value [5] of 37 ± 4 Å^2. Thus the $2-\sigma$ error bars overlap, although the result is suggestive of a slight increase with increasing temperature. A cross

section increasing with increasing temperature (i.e., increasing collision velocity) is produced by an interaction involving a repulsive wall or barrier. However, a large low temperature cross section suggests attractive forces, as noted above, and should lead to a decrease with temperature. A decrease appears ruled out by the present results. Possibly, two different parts of the interaction potential are sampled over this enormous and previously unexamined temperature range.

The intercept in Fig. 3 represents the decay of excited NO in the absence of NO quencher. Its value is $9.2 \pm 1.8\,\mu s^{-1}$, again $1-\sigma$ error. This is faster than the well-established [13, 14] purely radiative rate of $4.7\,\mu s^{-1}$. It can be interpreted as due to quenching by the N_2 present. If so, the corresponding cross section is $1.7\,Å^2$. At room temperature, the previously established cross section [5, 13, 14] is very small, $< 0.01\,Å^2$. Both a small low temperature value and an increase with temperature are consistent with quenching governed wholly by repulsive or barrier forces. Such a barrier could be explained [15] by a curve crossing involving an $NO^+N_2^-$ charge transfer complex and the neutral pair of molecules. An Arrhenius dependence on temperature drawn through the rate constants at 300 and 3500 K yields an activation energy of 4 kcal. This suggests a cross section of $1.3\,Å^2$ at 1700 K, which would make N_2 the third most important collider in methane/air flames at that temperature [7]. Other recent flame measurements [16] show a similar degree of quenching, also placing it third most significant after H_2O and CO_2. These results all indicate a sharp temperature dependence of σ_Q of NO $A^2\Sigma^+$ by N_2, in contrast to the negligible role often assumed owing to the extremely slow room temperature quenching. This result has important implications concerning the quantum yield at high temperature, in both chemiluminescent NO γ-band emission and LIF measurements of NO in flames and other systems, and is one example of a quenching mechanism involving an energetic barrier.

Acknowledgement. This research was supported by SDIO/IST under a contract managed by the U.S. Army Research Office.

References

1. L.C. Howlett, P. Espy, P. Erdman: Bow Shock Ultraviolet Quick Look Data Report, Utah State University Space Dynamics Laboratory Report SDL/90-042, June 1990
2. G.P. Smith,. D.R. Crosley, D.F. Eckstrom: Mechanism and Rate Constants for the Chemistry of Radiating, Shock-Heated Air, SRI International Report MP 89-037, February 1989
3. C. Park: Prog. Astro Aero. **96**, 395 (1985)
4. D.A. Levin: Private communication (1990)
5. G.A. Raiche, D.R. Crosley: J. Chem. Phys. **92**. 5211 (1990)
6. B.P. McMillin, M.P. Lee, P.H. Paul, R.K. Hanson: AIAA Paper 89-2566, Twenty-Fifth Joint Propulsion Conference, Monterey, California, July 1989
7. D.E. Heard, J.B. Jeffries, D.R. Crosley: Chem. Phys. Lett. (1991) in press
8. D.E. Heard, J.B. Jeffries, G.P. Smith, D.R. Crosley: submitted to Combust. Flame (1991)
9. R.E. Mitchell, R.J. Kee: A General Purpose Computer Code for Predicting Chemical Behavior Behind Incident and Reflected Shocks. Sandia National Laboratory Report SAND82-8205 (1982)
10. W.H. Wurster, C.E. Treanor, M.J. Williams: AIAA Paper 89-1918, Twentieth Fluid Dynamics, Plasma Dynamics and Lasers Conference, Buffalo, New York, June 1989
11. D.R. Crosley: J. Phys. Chem **93**, 6273 (1989)
12. R.J. Cattolica, T.G. Mataga, J.A. Cavolowsky: J. Quant. Spectrosc. Radiat. Transfer **42**, 499 (1989)
13. I.S. McDermid, J.B. Laudenslager: J. Quant. Spectrosc. Radiat. Transfer **27**, 483 (1982)
14. G.D. Greenblatt, A.R.Ravishankara: Chem. Phys. Lett. **136**, 501 (1987)
15. M. Asscher, Y. Haas: J. Chem. Phys. **76**, 2115 (1982)
16. M. Drake, J. Ratcliffe: Submitted to J. Chem. Phys. (1991)

Appendix D

LASER MEASUREMENT OF CHEMICALLY REACTIVE INTERMEDIATES IN COMBUSTION

D. R. Crosley, "Laser Measurements of Reactive Intermediates in Combustion," in Turbulence and Molecular Processes in Combustion, T. Takeno, Ed., Elsevier, Amsterdam, in press, 1992.

Laser measurement of chemically reactive intermediates in combustion

David R. Crosley, Molecular Physics Laboratory, SRI International, Menlo Park, California 94025

Abstract

Laser-induced fluorescence has reached maturity as an important tool in the study of combustion processes. It may be employed in several ways, to make pointwise distributions or planar images in turbulent flames, or spatial profiles above burners supporting laminar premixed flames. We review its use for the latter case, in a study of prompt NO formation in low pressure methane/air flames. Spectroscopic knowledge needed for LIF studies is considered and a developmental example of HCO is given. Finally, the important issue of collisional quenching, which dominates the fluorescence quantum yield in most flames, is discussed. As more quenching rates for different colliders and as a function of temperature become available, it appears that collisional quenching can be estimated well for many flame conditions. This is now the situation for OH, CH, NH, and NO. Experiments and calculations of quenching for HCO and NO are described.

LASER-INDUCED FLUORESCENCE IN COMBUSTION

The technique of laser-induced fluorescence has attained maturity in the field of combustion science. At the Twenty-fourth International Symposium on Combustion, held in Sydney in July 1992, 13% of the papers (oral plus poster) containing experimental investigations involved the use of LIF. In each case, LIF was utilized for the study of a combustion system or combustion-related chemical kinetics investigation. This contrasts with the situation a few years ago, when most or all of the LIF papers at a meeting would be concerned only with the demonstration or development of the LIF method itself.

LIF may be employed in several ways to study flames. In one, measurements are made of distributions of chemically active species in turbulent flow situations. An excellent example is given by pointwise measurements of OH together with Raman determinations of temperature and major species in piloted turbulent jet diffusion flames [1]. Conditional averages of mass fraction of different species showed that local mixture fraction and temperature could describe the chemical state of the flame system independent of mixing history, but the mixing characteristics could not be described by a series of steady laminar flame calculations. Two-dimensional, planar LIF imaging can also be used to yield instantaneous patterns of radical species in turbulent chemically reactive flows; as an example, see [2], where CH and OH were examined in a lifted turbulent jet flame. Images of these two radicals form particularly useful semiquantitative purposes [3]: CH serves as a marker of the flame front, and shows where the combustion reactions are occurring; whereas OH, ubiquitous in flames and easy to determine, is present at highest concentration in the burnt gases and therefore denotes where reaction has taken place. In

ELSEVIER SCIENCE PUBLISHERS B.V.

experiments such as these, one can use LIF to study the interaction between turbulence and chemistry in combustion.

On the other hand, a turbulent flame is too complex a system for the investigation of the fine details of the combustion chemistry itself. This is best accomplished via measurements in laminar flames, where LIF is used to obtain spatial (one- or two-dimensional) profiles of trace reactive species, made as a function of height above a burner surface. Absolute or relative profiles may be compared with the predictions of a large scale model of the combustion chemistry, which contains dozens of species and over a hundred reactions. Highly spatially resolved LIF determinations of key chemical intermediates in low pressure flames form excellent tests of such a model, ultimately establishing its ability to describe flames under conditions much more difficult to investigate. In this way, LIF ensures that the combustion chemical mechanism is more fully understood.

Finally, LIF may be used in a semiquantitative way, so that simply the detection of some species present at an approximate concentration can reveal a good deal of information about the chemical mechanism [4]. For example, the NS radical was detected in flames seeded with small amounts of nitrogen and sulfur compounds so as to mimic fuel-bound coal species [5]. This showed that a large fraction of the sulfur was tied up temporarily in this radical intermediate, indicating its importance in linking the chemistry of formation of both NO_x and SO_x pollutants. A possible future application of this approach might be detection of alkoxy or alkylperoxyl radicals of likely importance in ignition phenomena such as knock in internal combustion engines. Clearly, this semi-quantitative use of LIF detection could be applied to turbulent flames, where the presence of some species may suggest more detailed chemical mechanistic studies to be performed in laminar flow situations.

In what follows, we first review a flame chemistry study from our laboratory, in which LIF was used to measure temperature and species profiles for comparison with a model calculation investigating prompt NO formation in natural gas combustion. Conclusions are drawn concerning both the measurement process and our degree of understanding of the chemistry. We then turn to future needs of LIF development, examining through the example of HCO radical detection some necessary spectroscopy, and via NO measurement questions of collisional quenching.

PROMPT NO FORMATION IN METHANE/AIR FLAMES

Nitric oxide is formed during the combustion of all hydrocarbon fuels burning in air, including natural gas which is otherwise a relatively cleanly burning fuel. Environmental regulation, expected to become increasingly stringent in the future, has focused attention on this pollutant, so that its reduction is a crucial objective for many combustion situations. To understand the chemistry of formation of nitric oxide in natural gas combustion, we performed LIF measurements of trace reactive intermediates responsible in the so-called prompt NO cycle, and compared these with predictions from a computer model of the appropriate chemical networks [6].

Knowledge of the basic mechanistic steps allowed us to choose the species to be measured. The reaction sequence, first postulated by Fenimore [7], begins near the flame zone. There, reaction between the CH radical and N_2 from the air forms N atoms and HCN molecules. The N atoms react with O_2 and OH to directly produce NO; the HCN undergoes a series of oxidation steps to produce another N atom and hence another NO molecule. The levels of NO produced in premixed natural gas flames are often tens of

ppms, levels similar to that of the reactive radical species. Therefore a sensitive test of the mechanism must involve measurements of these species at high spatial resolution: CH as the main precursor, NO as the direct pollutant of interest, and OH (and/or H atoms) as markers of the flame chemistry.

The measurements were made in a low pressure flame facility designed for laser probing. The burner was a 6 cm diameter McKenna porous plug burner, surrounded by an Ar shroud flow. Rapid flows lifted the flame 1 to 2 cm off the burner at the operating pressure of 30 Torr, providing adequate spatial resolution below and in the flame front where much of the interesting and relevant chemistry occurs. The laser beam was directed across the burner and the fluorescence collected at a right angle; the burner was translated vertically to trace out profiles of species concentrations vs height above the burner, transformable into reaction time by knowledge of the gas flow rates.

LIF profiles for four different species are shown in Fig. 1. Only relative values of CH and H were determined, but OH and NO were measured absolutely. OH was calibrated by direct absorption, and NO by flowing room temperature NO in helium through the burner chamber; quantum yield corrections for quenching were made when necessary using direct lifetime measurements.

A profile of the temperature through the flame forms a key input to the chemical model. Our experience shows that it must be determined accurately and with a high degree of spatial precision relative to the species profiles that are to be compared with the model predictions. Because of the highly nonlinear dependence of chemical reaction rate coefficients on temperature, an apparent temperature determination that is 100K different from the true value can render meaningless a quantitative comparison between model and experiment.

Therefore we have also chosen LIF as the means of temperature measurement in these laminar flames, as it furnishes the same spatial resolution and fidelity as the species determinations. Temperature is determined using rotational excitation scans through a compact 4 Å region of the spectrum of the OH radical containing rotational levels spanning an energy range of 4000 cm^{-1}. For accurate temperatures, attention must be paid to the spectral bandpass and temporal gating of the

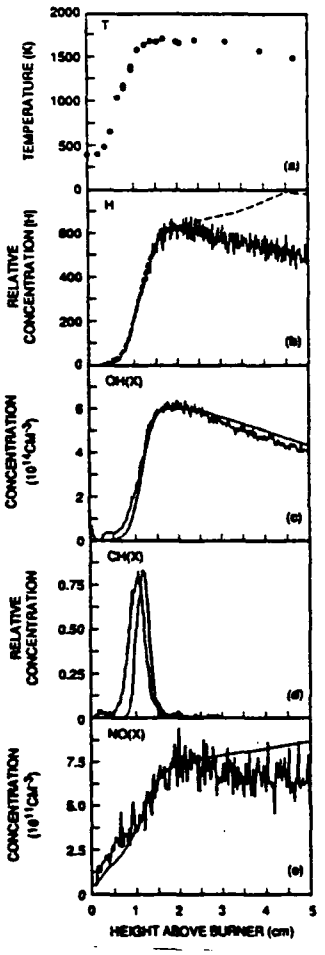

Figure 1. Spatial profile results from the 30 Torr methane/air flame at a mixing ratio of 1.13. The smooth lines are the model predictions. a) Temperature profiles determined by LIF excitation scans in OH. b) H atom measurements from two-photon LIF. c) OH concentration; the model is scaled by a factor of 0.67 to match the experiment. d) Relative CH concentration. e) Absolute NO concentration.

detection apparatus [8]. Such a scan is shown in the top panel of Fig. 2. These data can be analyzed in two ways, which weight the data slightly differently. First, a Boltzmann plot may be made of the populations of each rotational level, taken from the peak line intensities and the appropriate rotational transition probabilities. This is shown in the lower panel of Fig. 2. Second, the spectrum may be directly simulated using temperature as an input parameter, varying the temperature to obtain the best fit between simulation and experiment. The residual from such a fit is also shown in the top panel. Tests showed that these two approaches to the data analysis yielded the same temperatures to within experimental error, which was typically ± 30 to 40K at 1700K. A spatially resolved temperature profile determined with these scans is shown in the top panel of Fig. 1.

The computer model of the flame chemistry is based on the Sandia laboratory one-dimensional flame code [9], with a mechanism containing nitrogen-chemistry rate constants largely based on the review by Miller and Bowman [10]. 38 species and 148 reactions are included. The temperature profile is input to the model, a procedure preferable to regarding temperature as one of the outputs. The computed species concentrations are also shown in Fig. 1. Note that the H atom profile matches well through the flame front region, even though it diverges in the burnt gases (this divergence is partly but not wholly due to radial flame spread and diffusion [11]). The OH profile, however, is well matched everywhere. The computed value has been scaled here by a factor of 0.67 to correspond to the measured absolute value, although the difference from unity is within measurement error bars. For CH, only relative profiles were determined. The computed profile is of the proper width and shape, but rises late in the flame compared with experiment, a mismatch that has important consequences for our ability to predict NO, as discussed below. The bisigmoidal shape of the NO profile below the flame front is due to backward diffusion of NO formed near the flame front, and is reproduced by the model. The absolute values from calculation (3.7 ppm) and experiment (4 ppm) agree within error bars.

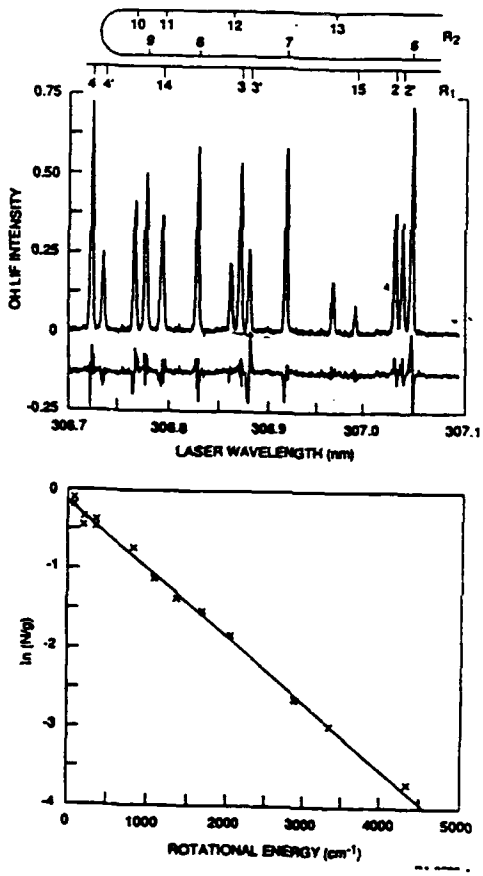

Figure 2. Top: OH rotational excitation scan in the methane/air flame. The residual from the fit, which yielded 1701K, is shown below the spectrum. Bottom: Boltzmann plot from the intensities in the top trace; the fit yields 1732 ± 32K.

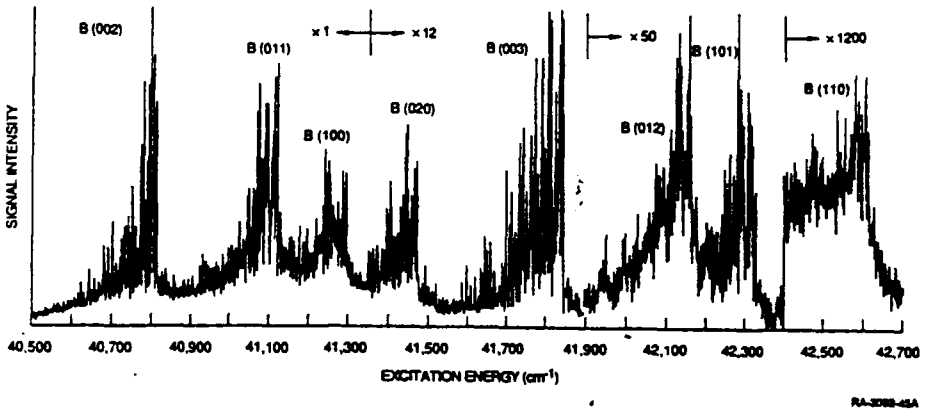

Figure 3. Excitation scan for the $\tilde{B}$ - $\tilde{X}$ system of the HCO radical in a photolysis cell. This broad wavelength range covers eight bands at 1.2 cm^{-1} resolution. Note the sensitivity changes.

The reasonable agreement between experiment and model predictions indicates that we understand prompt NO chemistry rather well, and can describe it using the key reactions and rate constants found in Miller and Bowman [10]. In particular, NO itself is in excellent agreement. However, the CH profile is not in such good agreement. Senstivity analysis shows a nearly unit sensitivity of NO concentration to the CH + N_2 reaction, i.e., doubling the net rate of this reaction will double the computed NO. Therefore, if CH is not predicted properly, we can't expect to predict NO accurately. Furthermore, this key reaction has a very strong temperature dependence, so that it is important to know the profile of CH relative to the steep temperature gradient in the reaction zone. Therefore we must regard the success for NO with some caution.

Although the chemical kinetic mechanism is reasonably well understood quantitatively, part of the agreement must be considered fortuitous. We cannot yet with confidence predict NO for other flame conditions (e.g., different fuel/air mixing ratios) where the relationship between CH and temperature profiles may be different. Future experiments at different initial stoichiometries should help sort out this question. Note the importance, in reaching this conclusion, of measuring not just the NO itself, but also the CH radical, its major precursor.

SPECTROSCOPIC STUDIES FOR LIF DIAGNOSTICS

Laser-induced fluorescence is not a universal technique, like mass spectroscopy. It is limited to those molecules that absorb laser light in an available and usable wavelength region. In particular LIF is ill suited for the measurement of closed shell molecules that have very highly energetic excited states, lying in the vacuum ultraviolet. That category includes many fuel, oxidant and exhaust gas molecules (CH_4, H_2, N_2O, CO_2, H_2O, and N_2) present as major species in combustion systems (these molecules are often detected nonintrusively by Raman scattering methods).

However, there is a very large number of intermediate species, including many free radicals, that are amenable to LIF detection, having electronic levels or band systems in suitable wavelength regions. They are usually present in only minor or trace amounts, so

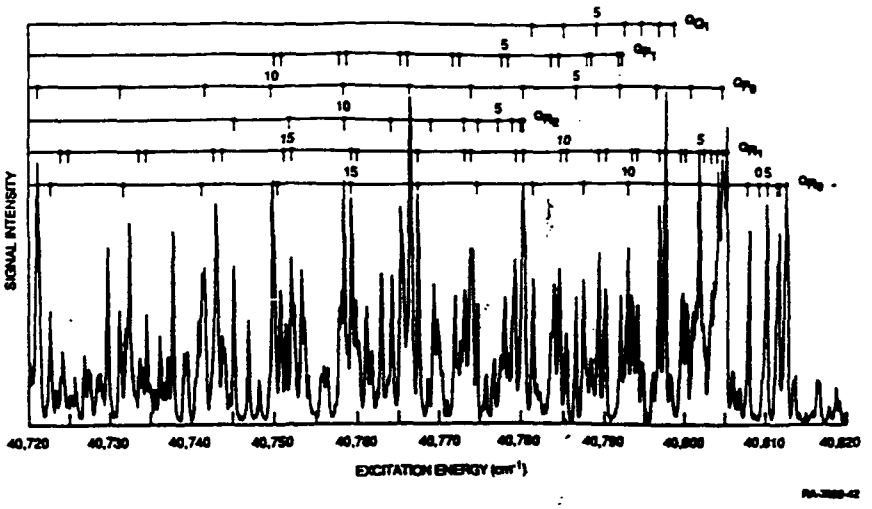

Figure 4. Excitation scan of the 002 - 000 band of the $\tilde{B}$ - $\tilde{X}$ system of HCO in photolysis cell at 0.06 cm^{-1} resolution. Six of the assigned rotational branches are marked. Weaker branches of this hybrid band exist to the blue Q_{R0} bandhead.

that the sensitivity afforded by LIF is important in their detection, and the questions addressed by their measurement usually concern aspects of combustion chemistry. In Table I are listed combustion-related species, containing 1 to 4 atoms, which have been detected using LIF. The list is restricted to molecules composed of the five atoms H, O, C, N, and S, that occur naturally in many fuels. Note that the first entries on the list. the free atoms, have their first resonance absorption transitions in the vacuum ultraviolet, and they are detected using two-photon LIF. Simultaneous absorption of two laser photons in the near ultraviolet elevates the atom to a high-lying excited state, from which it radiates (in the visible or infrared) to another excited state. Two-photon LIF is also the means of detection of CO and NH_3 as trace species.

Each of the entries in Table I has an important spectroscopic characteristic. The absorption spectra for each atom or molecule comprise distinct and identifiable line absorption patterns. Examples are seen in Fig. 2 and in Figs. 3 and 4 discussed below. This is crucial to the selectivity of LIF, in order for each molecule to be distinguished in the presence of other possible absorbing features in the same wavelength region. Often, different but important intermediate species can be present in concentration ratios of two to four orders of magnitude, so that these spectroscopic fingerprints are essential to the identification of the molecule present at the lower concentration.

In addition to the species listed in Table I, there are many other combustion-related species that can be made to fluoresce with a laser. These include: many metal atoms and their compounds, often found as impurities in fuels; species present in special combustion

Table I
Combustion Chemistry Intermediates Detectable by Laser-Induced Fluorescence

Molecule[a]	Excitation wavelength (nm)	Molecule[a]	Excitation wavelength (nm)
H*	206	NCO*	440
C*	280	HCO*	245
O*	226	HCN	189
N*	211	HNO	640
S	311	NH_2*	598
OH*	309	C_3	405
CH*	413	C_2O	665
NH*	336	S_2O	340
SH*	324	SO_2*	320
CN*	388	NO_2*	590
CO*	280	HSO	585
CS	258	CS_2	320
NO*	226	N_3	272
NS*	231	NCN	329
SO*	267	CCN	470
O_2*	217	NH_3*	305
S_2*	308	NO_3	570
C_2*	516	C_2H_2*	220
$^1CH_2$*	537	CH_2O*	320

[a] An asterisk demotes that LIF detection has been performed in a flame.

23 cm

systems, such as boron compounds in energetic materials or chlorine containing radicals in chlorinated hydrocarbon waste incineration; polyaromatic hydrocarbons, important in soot formation; partially oxygenated hydrocarbons, such as aldehydes, that are intermediates in the oxidation process; and larger hydrocarbon fuels, including ethylene and isooctane. Whereas the metals, boron compounds, and chlorinated radicals do have distinct line spectra, most of the hydrocarbon species do not, and their identification in a combustion system, while quite useful, must be approached with care.

Table I contains a large fraction of the small intermediate, reactive species that are important in combustion chemistry. Thus LIF has the ability to form a quite complete characterization of a combustion chemical mechanism. A few other entries would be desirable: of particular interest would be LIF detection of $^3CH_2$, HO_2, C_2H, and CH_3, although suitable fluorescing electronic transitions are not known at this time.

As an example of the development of the LIF spectroscopy of an important combustion intermediate, we consider the HCO radical. HCO is formed partway along the methane oxidation path, through the unimolecular or bimolecular destruction of formaldehyde. It reacts in several ways. Unimolecular decomposition produces a reactive hydrogen atom, while bimolecular reaction with O_2 yields a relatively unreactive HO_2 radical, slowing the flame. Reaction with H, OH or O compete with the decomposition; these reactions remove species from the reactive H/O radical pool. Thus the relative rates of these reactions is important in controlling the net rate of H atom production in the flame and hence chain propagation and the flame speed. Accordingly, measurement of HCO is an important test of our understanding of combustion chemistry, especially the kinetics of the ignition process.

Although HCO has been detected in flames with both mass spectroscopy and resonant multiphoton ionization, a fully nonintrusive optical method is desirable. HCO possesses two known electronic band systems. The $\tilde{A}$ - $\tilde{X}$ system in the visible is well known in absorption, but the rapid predissociation of the $\tilde{A}$ state renders its fluorescence too weak for useful flame detection. The $\tilde{B}$ - $\tilde{X}$ system in the ultraviolet has been known for years in emission as the hydrocarbon flame bands, but it had been observed in absorption only from HCO produced on a 14K Ar matrix.

We undertook experiments to establish laser-induced fluorescence detection of HCO in the $\tilde{B}$ - $\tilde{X}$ system, and to examine its utility as a flame diagnostic tool. LIF spectra were first found forming HCO by the photolysis of slowly flowing acetaldehyde in a room temperature cell [12]. An excitation spectrum showing several bands of this electronic system is shown in Fig. 3. Note the gain changes throughout this broad scan; fluorescence from the 110 level is three orders of magnitude smaller than the 002 level. This is certainly due to the rapid increase of predissociative rate, and concomitant decrease in quantum yield, with increasing $\tilde{B}$ state vibrational energy. A portion of the 002 - 000 band is shown at much higher resolution in Fig. 4, with the appropriate rotational assignments for this asymmetric rotor transition. Understanding this line pattern and its assignment is crucial to identification in a flame. Fluorescence spectra provide further identification, as well as establishing vibrational constants for the ground electronic state.

Based on this spectroscopic study, HCO was soon detected with LIF in a 6 Torr methane/oxygen flame [13]. Identification was made using the assigned excitation scan of the 002 - 000 band, and confirmed through fluorescence spectra. The fluorescence spectra revealed the overlap of this HCO excitation band with part of the 3-0 band of the A-X system of OH. A profile of the HCO LIF intensity through the flame is shown in Fig. 5, and compared with calculations for this flame [14]. Conversion of LIF intensity to HCO concentration for proper comparison requires knowledge of the collisional quenching, not available at the time the flame study was made. This was subsequently

measured using direct time decay of fluorescence in the 000 - 000 band [15]. Applied to this flame (see the next section) these results indicate that the quenching and thus the quantum yield is nearly constant over the region where the HCO exists in this low pressure flame. Future studies designed to make HCO detection more quantitative include measurement of the transition probabilities for individual bands, and the temperature dependence of quenching.

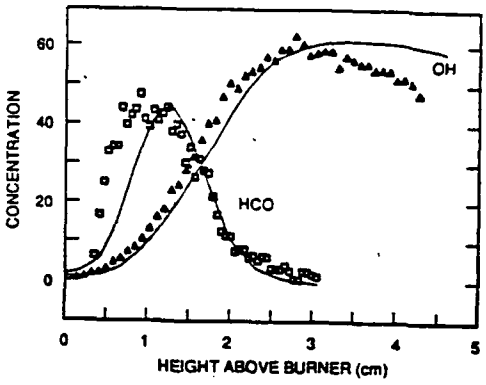

Figure 5. Profile of the HCO radical above the burner in the 5.7 Torr methane/oxygen flame, together with the model predictions from Ref. 14. The OH experimental and predicted profiles are also shown for comparison.

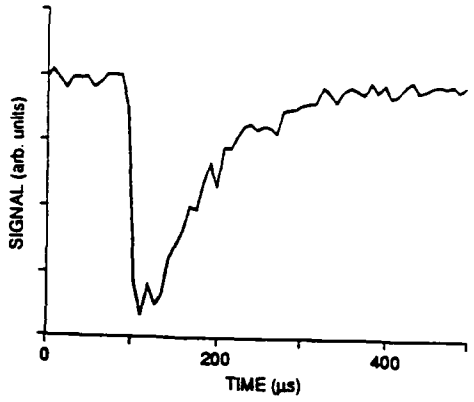

Figure 6. Single-shot LIF decay trace for NO in a shock. The negative-going signal denotes detection of light in the photomultiplier. In this case, the shocked gases are at a temperature of 3400K and consist of 0.83 Torr NO and 41 Torr N_2.

COLLISIONAL QUENCHING IN FLAME LIF

Because the excited, emitting state created by the laser lives for a finite time period, it is subject to the influence of collisions. These may transfer it among internal rotational and/or vibrational levels of the electronically excited state, or remove it altogether so that radiation does not occur. This latter process, called quenching, is the main factor in determining the fluorescence quantum yield, that is, the fraction of excited molecules that emit radiation. The quantum yield is needed to correctly relate the number of emitted photons to the desired concentration of the ground state species originally responsible for the absorption of the laser radiation. For example, for each thousand excited OH molecules in an atmospheric pressure flame, only two will emit a photon and the remainder will be collisionally quenched.

Even if one desires only relative concentrations, for example as a function of burner height as in Figs. 1 and 5, or throughout an instantaneous image in a turbulent flame, knowledge of the quenching is necessary. For this purpose one needs to know the major species flame gas composition and the temperature at each point of measurement. These must be combined with quenching cross sections for each collider gas as a function of

temperature. For laminar flames, adequate composition information is provided through chemical model calculations. For a turbulent flame, separate measurements (e.g., via Raman scattering) will furnish the major species concentrations. Quenching cross sections have been measured for several of the species in Table I, although seldom as a function of temperature. Only for OH, CH, NH and NO does an adequate temperature-dependent quenching data base exist to estimate the quantum yield under combustion conditions, although these species are by far the most popular molecules for LIF studies.

There are two examples in which LIF signals in OH have been corrected for collisional quenching using measured major species compositions and temperature dependent cross sections. The first consists of pointwise measurements in turbulent jet diffusion flames, whose results were discussed earlier. The quenching corrections were made in the following way [16]. For each instantaneous point measurement, major species concentrations and temperature were determined using Raman scattering, together with the OH LIF signal intensity. These compositions and temperature were then used together with OH quenching cross sections tabulated as a function of temperature for colliders of importance in combustion [17] to calculate the quenching for each measurement. Quenching corrections to the OH LIF intensity data were then plotted as functions of overall mixing ratio and temperature. A survey of these results indicates that knowledge of those two parameters alone allowed a prediction of the correct quenching to within perhaps 10%, without independently measuring all compositions; and in any event, the quenching correction was rarely greater than about 30% from measurement to measurement. The second example consists of methane/air diffusion flames burned on a Wolfhard-Parker slot burner [18]. Major species profiles had been determined for this flame using mass spectrometric probing, and were combined with the same temperature dependent, collider-specific quenching cross sections from Ref. 17. The results showed that, although there was a potential variation in quenching rate of a factor of five between the cold fuel and air regions of the burner, the quench rate varied only 20% from the mean in the hot portion of the flame where the OH was found. These examples of small variation in OH quenching rate with flame position were also suggested by an examination of flame compositions reported in the literature [17]. This is encouraging in that, if there is but little variation in quench rate, then errors introduced in an estimation of the quench rate are quite small indeed. As a result, with current knowledge at least of OH cross sections, we might reasonably expect absolute quantum yield estimates for OH good to within better than 30% at any point, and relative values close to 10% accuracy.

This approach using calculated species concentrations [14] and measured room temperature quenching [15] has been applied to estimate HCO quenching rates noted for the low pressure methane/oxygen flame in the preceding section. Several assumptions were made: the cross sections at room temperature are valid for higher temperature; cross sections for H_2O and CO are taken equal to the values measured for NH_3 and N_2, respectively; and quenching for the 002 level (observed in the flame) is the same as for the 000 level measured in the laboratory. The result shows a 4% variation in quench rate proceeding from 0.7 to 1.7 cm height above the burner (see Fig. 5), covering the range of most of the HCO concentration. The major questions here are the actual H_2O quench rate (this is difficult to measure and we have previously considered NH_3 as a surrogate collider in just this way), and the temperature dependence of the quenching cross sections. Nonetheless, this simple calculation provides confidence that the LIF intensity profiles for HCO [13] are realistic profiles of its actual concentration.

The interest in controlling the emission of NO has made this species a popular target for LIF studies, both pointwise and more recently in imaging. Therefore knowledge of its collisional quenching is important. Until a short time ago, measurements only existed

at room temperature; some cross sections were quite large, suggesting the influence of attractive forces in the collisional process and a concomitant decrease in cross section with increasing temperature, as found for OH and NH [19]. Measurements made in a heated cell [20] showed that this analogy did not hold: quenching by H_2O did decrease with temperature, but quenching by O_2 and NO itself did not. Quenching by N_2 was so small at room temperature as to be ignored.

These cross sections were used to calculate the NO quenching rate at different positions in the low pressure methane/air flame, for comparison with direct time dependent decay measurements [21]. The major species concentrations were obtained from the model calculations. The results showed excellent agreement, that is, the calculated absolute quenching was within 20% of that measured. However, the temperature dependence of quenching by other gases was not known at the time.

Since then, several experiments in different laboratories have been performed to investigate the quenching of NO at higher temperature. The first was a measurement in a shock tube at high temperature, near 3500K [22]. A single pulse of the laser could be fired in each shock; an example of the resulting fluorescence decay trace is shown in Fig. 6. From this is obtained a quenching rate, through measurements at different NO/N_2 ratios. Of particular interest was the finding that N_2 quenched NO appreciably at high temperature, despite its inability to do so at room temperature. This meant that N_2 must be considered as an important quencher in air-based flames at high temperatures. Further measurements in a heated cell [23] confirmed this result and provided temperature dependent cross sections for other species. Finally, a recent, more comprehensive shock tube experiment has investigated quenching due to CO_2 [24] and N_2 [25].

We can use these new quenching cross sections to improve the calculated quenching rate for NO in the 30 Torr flame. The only changes of significance compared with the calculation in Ref. 21 are a reduced high temperature cross section for CO_2 (to 75% of the value used previously) and a doubling of the CO cross section. Importantly, the N_2 and H_2O values are confirmed by the more recent work. This reduces the calculated quenching rate from that in Ref. 21 by 2% at 1190K and by 8% at 1680K, and the new values remain in good agreement with experiment. Thus knowledge of the collisional quenching of NO by flame gases appears in good shape, due to recent interest in and attention to this important species.

CONCLUSION

Laser-induced fluorescence has reached maturity as a tool for the understanding of combustion chemistry. It can be applied to a many trace species which are reactive flame chemical intermediates, covering a large fraction of those intermediates found in models of that chemistry. Collisional quenching at different positions in the flame must be known for quantitative measurements and comparisons with those detailed models, but the ability to calculate quenching rates appears quite good for those species for which exist quenching rate coefficients (OH, CH, NH and NO).

ACKNOWLEDGEMENTS

In this short review I have described parts of many experiments, which involved a large number of coworkers. I wish to especially thank Jay Jeffries and Greg Smith for our continuing collaboration on LIF flame studies, and also Don Eckstrom, Dwayne Heard, Lukas Hunziker, Ulrich Meier, George Raiche, Andy Sappey, and Ingrid Wysong

for their participation in various experiments. The research described was supported by the Physical Sciences Department of the Gas Research Institute, by the Southern California Gas Company, by the Air Force Office of Scientific Research, and by the Strategic Defense Initiative Office through the Army Research Office.

REFERENCES

1. R. S. Barlow, R. W. Dibble, S. H. Stårner, and R. W. Bilger, Twenty-Third Symposium (International) on Combustion, The Combustion Institute, Pittsburgh, 1990, p. 583.

2. R. W. Schefer, M. Namazian, and J. Kelly, Twenty-Third Symposium (International) on Combustion, The Combustion Institute, Pittsburgh, 1990, p. 669.

3. M. J. Dyer and D. R. Crosley, Proceedings of the International Conference Lasers '84, STS Press, McLean, Virginia, 1985, p. 211.

4. D. R. Crosley, Comb. Flame **78**, 153 (1989).

5. J. B. Jeffries and D. R. Crosley, Comb. Flame **64**, 85 (1986).

6. D. E. Heard, J. B. Jeffries, G. P. Smith and D. R. Crosley, Comb. Flame **88**, 137 (1992).

7. C. P. Fenimore, Thirteenth Symposium (International) on Combustion, The Combustion Institute, Pittsburgh, 1971, p. 373.

8. K. J. Rensberger, J. B. Jeffries, R. A. Copeland, K. Kohse-Höinghaus, M. L. Wise and D. R. Crosley, Appl. Opt. **28**, 3556 (1989).

9. R. J. Kee, J. F. Grcar, M. D. Smooke and J. A. Miller, Sandia National Laboratory Report SAND85-8240 (1985).

10. J. A. Miller and C. T. Bowman, Prog. Engr. Comb. Sci. **15**, 287 (1989).

11. J. B. Jeffries, G. P. Smith, D. E. Heard, and D. R. Crosley, Ber. Bunsenges. Phys. Chem. **96**, xxxx (1992).

12. A. D. Sappey and D. R. Crosley, J. Chem. Phys. **93**, 7601 (1990).

13. J. B. Jeffries, D. R. Crosley, I. J. Wysong, and G. P. Smith, Twenty-Third Symposium (International) on Combustion, The Combustion Institute, Pittsburgh, 1990, p. 1847.

14. G. P. Smith, Paper 92-98, Western States Meeting of the Combustion Institute, Berkeley, California, October 1992.

15. U. E. Meier, L. E. Hunziker, and D. R. Crosley, J. Phys. Chem. **95**, 5163 (1991).

16. R. S. Barlow, R. W. Dibble, S. H. Stårner, and R. W. Bilger, Paper 89-106, Western States Meeting of the Combustion Institute, Livermore, California, October 1989.

17. N. L. Garland and D. R. Crosley, Twenty-First Symposium (International) on Combustion, The Combustion Institute, Pittsburgh, 1988, p. 1693.

18. K. C. Smyth, P. J. H. Tjossem, A. Hamins, and J. H. Miller, Comb. Flame **79**, 366 (1990).

19. D. R. Crosley, J. Phys. Chem. **93**, 6273 (1989).

20. G. A. Raiche and D. R. Crosley, J. Chem. Phys. **92**, 5211 (1990).

21. D. E. Heard, J. B. Jeffries, and D. R. Crosley, Chem. Phys. Lett. **178**, 533 (1991).

22. U. E. Meier, G. A. Raiche, D. R. Crosley, G. P. Smith, and D. J. Eckstrom, Appl. Phys. B **53**, 138 (1991).

23. M. C. Drake and J. W. Ratcliffe, General Motors Research Laboratory Report GMR-7426, July 1991.

24. J. A. Gray, P. H. Paul, and J. L. Durant, Chem. Phys. Lett. **190**, 266 (1992).

25. J. W. Thoman, J. A. Gray, J. L. Durant, and P. H. Paul, J. Chem. Phys., submitted, 1992.

23 cm